



# Green Synthesis of Metal Nanoparticles Using *Cinnamomum*-Based Extracts and Their Applications

Omar Samir Mohamed Megahed Saleh Elmitwalli, Deyari Azad Kareem Kassim,  
Ahmed Taymour Algahiny , Fryad Zeki Henari 

Department of Medical Sciences, Royal College of Surgeons in Ireland - Medical University of Bahrain, Busaiteen, Muharraq, Kingdom of Bahrain

Correspondence: Ahmed Taymour Algahiny, Email 19201282@rcsi.com

**Introduction:** Nanotechnology is the science that deals with matter on the nanoscale, with sizes ranging from 1 to 100 nm. It involves designing, synthesising, characterising and applying these nanoscale materials. Nanoparticles (NPs) are known for their high surface-area to volume-ratio, surface charge density, low melting point, and distinguishably good optical/electrical properties. NPs exhibit an excellent drug delivery system, an effective contrast agent for vascular imaging, and effective antimicrobial activity. The biological synthesis of NPs is a simple, cost-effective, and environmentally friendly technique. This bottom-up technique utilises organisms' enzymes/bio-compounds and a plant extract as capping and reducing agents. *Cinnamomum* species are known for their intrinsic antimicrobial, antidiabetic, antioxidant, anti-inflammatory, anticancer, and neuroprotective properties. This review summarises articles that greenly synthesised NPs using *Cinnamomum* species' extracts, describing their methodologies, characterisation of the nanoparticles and their medical applications.

**Methods:** A literature search has been conducted on databases PubMed, ScienceDirect, and Frontier on the green synthesis of metal nanoparticles (MNPs) using *Cinnamomum*-based extracts. Various articles reported the methodology of utilising *Cinnamomum* species' extracts as reducing and capping agents. Only original lab articles were considered.

**Results:** Various types of MNPs have been successfully synthesised. The most common *Cinnamomum* species utilised as extracts is *Cinnamomum tamala*. The most common applications tested were the MNPs' antibacterial, antiviral, antifungal, antidiabetic and anticancerous activity. MNPs also had a role in treating mice-induced polycystic ovarian syndrome and Parkinson-like neurodegenerative diseases.

**Conclusion:** *Cinnamomum* species have been successfully utilised in the green synthesis of various MNPs. Silver and Gold NPs were the most reported. These MNPs proved their efficacy in multiple fields of medicine and biology, especially their antibacterial, antiviral and antifungal activity. Notably, the newly synthesised NPs showed promising results in treating polycystic ovarian syndrome in rats.

**Keywords:** green synthesis, *Cinnamomum*, metal nanoparticles, biological applications

## Introduction

Nanotechnology is considered the most dynamic and mushrooming field of research in material sciences.<sup>1</sup> It is universally the subject of interest in transitional research.<sup>2</sup> Nanotechnology is the science that deals with matter on the nanoscale, with sizes ranging from 1 to 100 nm.<sup>1-3</sup> It involves designing, synthesising, characterising and applying these nanoscale materials.<sup>3</sup> Nanotechnology has been integrated enormously into medical applications such as drug and gene delivery, detection of proteins, pathogens and tumours and magnetic resonance imaging (MRI).<sup>3</sup> The variety of applications of nanoparticles (NPs) is attributed to their wide range of size distributions, large surface area, and morphology, which determines their novel or enhanced properties.<sup>4,5</sup> Metal nanoparticles (MNPs) are considered the most promising nanostructures to be utilised in the aforementioned medical applications.<sup>6</sup>

The synthesis of NPs can be divided into two main categories: top-down and bottom-up.<sup>7</sup> Each category includes several methods of synthesis. The green synthesis of nanoparticles is a bottom-up technique.<sup>7</sup> This technique has received increasing attention over the last decade, particularly in synthesising MNPs, due to the growing need to develop environmentally friendly, cost-effective, and relatively straightforward synthesis approaches.<sup>6–8</sup> In this process, living organisms such as plants, bacteria, algae and fungi are utilised to produce an extract that serves as reaction media and a capping agent.<sup>9</sup> The active biomolecules involved in these extracts are carbohydrates, proteins, vitamins, polymers, phytochemicals and natural surfactants, providing the NPs with a high state of stability and enhanced dispersity.<sup>10</sup> The other main category of techniques is the top-down techniques, including thermal decomposition, mechanical milling, lithography, laser ablation and sputtering.<sup>7</sup> The green synthesis of NPs is considered the best and the most promising synthesis approach compared to its chemical and physical counterparts. These chemical and physical approaches involve using hazardous and highly toxic chemicals and utilising costly instrumentation.<sup>7</sup>

The *Cinnamomum* species have been used as food derivatives and medicinal herbs for thousands of years. They are considered among the most popular medicinal herbs in the world in terms of their antioxidant capabilities, as they contain various polyphenolic compounds.<sup>11</sup> *Cinnamomum* has been shown to exhibit antibacterial and antifungal properties that can be useful in many ways. Cinnamon essential oils, for example, do not induce antimicrobial resistance, which allows them to be used for a long period of time.<sup>12</sup> *Cinnamomum verum*, an ancient spice, was widely used to flavour cooking, stewed fruit, and tea. Drinking *C. verum* tea regularly may help alleviate oxidative stress-related illnesses. It was also known for its medicinal benefits for diabetes and lowering blood cholesterol.<sup>13</sup> *Cinnamomum* species are commonly used in China to treat inflammatory diseases such as arthritis, skin-inflammatory, and diabetes-related inflammation.<sup>14</sup> *Cinnamomum* and its derivatives were observed to have anticancerous properties by various mechanisms including inhibiting nuclear factor-kappa B (NF-kB) and inducing apoptosis in cancer cells.<sup>12,15,16</sup> Due to their reducing and capping properties, *Cinnamomum* species are considered one of the best agents for synthesising MNPs.<sup>13</sup> It was reported in the synthesis of many MNPs, such as silver,<sup>14</sup> gold,<sup>17</sup> copper,<sup>18</sup> metal oxide, and magnetic<sup>13</sup> nanoparticles.

In this review, we briefly describe what NPs are, their classification (particularly MNPs), their synthesis, and the characterisation methods of these NPs. We then provide a detailed description of the literature available on MNPs that are greenly synthesised by utilising *Cinnamomum* species and their application. We will describe in detail the methodology of reports found on the topic, along with the summary of finding results related to the characterisation of these nanoparticles and their applications. This review should serve as a guideline and a reference paper for methodology, characterization, and biological/medical application in all *Cinnamomum*-related metal nanoparticles.

## Nanoparticles, Their Properties, Synthesis and Characterisation

### Nanoparticles and Their Properties

Nanoparticles are materials with nanoscale dimensions ranging from 1 nm to 100 nm.<sup>19</sup> A nanoparticle consists of three distinct layers: (i) the surface layer, to which metal ions, surfactants, polymers and small molecules attach.<sup>20</sup> (ii) The shell layer is a layer that protects against oxidation and other harsh environmental conditions.<sup>20,21</sup> (iii) The core involves the inner, central part of the NP, the part with which the NP is named.<sup>20</sup> NPs have unique optical properties that distinguish them from other materials. Their optical properties are size-dependent and manifest in a UV-visible excitation band absent in the bulk material.<sup>20</sup> This excitation band is known as the NP's Localised Surface Plasmon Resonance (LSPR). It arises from a collective oscillation of the conduction band electrons of the MNPs excited by the incident of a selective wavelength. The classification of NPs can be based on their size, morphology, and chemical or physical properties. There are four main types of NPs based on their chemical and physical characteristics: (a) Carbon-based NPs, (b) Metallic NPs, (c) Ceramic NPs, (d) Semiconductor NPs, (e) Polymeric NPs, (f) Lipid-based NPs.<sup>20</sup> In this review, we will highlight the role of *Cinnamomum* in developing MNPs.

### Metallic Nanoparticles

MNPs are the most studied types of nanoparticles.<sup>22</sup> They are synthesised purely from metal precursors. MNPs are composed of a metal core consisting of an inorganic metal or a metal oxide that is usually shielded by a shell of either

organic or inorganic material or metal oxide.<sup>20</sup> MNPs are an essential research focus due to their high surface area-to-volume ratio, pore size, surface charge and surface charge density, crystalline and amorphous structures, low melting point, good catalytic and thermal properties, and most importantly, their good distinguishable optical and electrical properties.<sup>13,23</sup> MNPs have unique LSPR features and possess distinguishable optoelectrical properties.<sup>20</sup> MNPs made of alkali and noble metals have a broad absorption band that is situated within the visible region of the electromagnetic spectrum.<sup>20</sup> Commonly used metal nanoparticles are gold (Au), silver (Ag), iron (Fe), zinc (Zn), copper (Cu), cobalt (Co), and aluminium (Al). MNPs can be prepared in various shapes and sizes. Zero-dimensional nanoparticles, quantum dots, nanospheres. One-dimensional nanorods, nanowires. Two-dimensional gold NPs are nanostars, and three-dimensional gold nanoparticles are triangular, nano-prisms, nanotubes, nanocubes, nano-dumbbells, and nano-dendrites.<sup>24</sup> By utilising all these unique properties of the MNPs, various applications can be established in different interdisciplinary branches, including medicine, agriculture, food, space, material science, biology, chemistry and physics.<sup>13</sup>

## Synthesis of Nanoparticles

Various methods and approaches can synthesise NPs. They can be synthesised physically by microwave irradiation, ultraviolet radiation, laser ablation, thermal decomposition, photochemical or radical-induced.<sup>25</sup> NPs can also be synthesised chemically by coprecipitation, supercritical fluid and chemical reduction.<sup>25</sup> Furthermore, biological approaches use bacteria, algae, fungi or plant extracts.<sup>25</sup> The synthesis of NPs can be subdivided into two main categories: (i) Top-down synthesis and (ii) Bottom-up synthesis.<sup>20</sup> Each category is subdivided into sub-categories or methods based on the procedure, the reaction's condition, and the adopted protocol. Figure 1 illustrates the various subdivisions and methods followed in synthesising NPs.<sup>20</sup>

The top-down synthesis employs a destructive approach in which a larger molecule is disintegrated into smaller molecules that are then modified and changed into NPs.<sup>22</sup> Mechanical milling is the famous and most studied example of a top-down method.<sup>23</sup> In this approach, a powder charge and a milling medium are placed in a high-energy mill to mill and blend the particle to a specific minute and controlled size and shape.<sup>26</sup> In mechanical milling, modifying factors such as plastic deformation, cold-welding and fracture can lead to a controlled change in the nanoparticle's parameters such as shape, an increase or a decrease in size, respectively.<sup>26</sup> This method has been utilised to synthesise many NPs, such as iron oxide NPs,<sup>27</sup> chalcopyrite (CuAlS<sub>2</sub>) NPs,<sup>28</sup> Zirconium Carbide (ZrC) and Hafnium Carbide (HfC) NPs.<sup>29</sup>

The bottom-up approach, also called the building-up approach, is the most common approach for synthesising NPs.<sup>20,30</sup> It involves building materials to construct the NPs.<sup>20,30</sup> Various techniques are based on a bottom-up approach, such as spinning, the sol-gel method and most importantly, the biological synthesis method.<sup>20,23,31</sup> In the spinning approach, a spinning disc reactor contains a rotating disc filled with the NP's liquid precursor. The reactor is filled with an inert gas to remove the oxygen within the rotator. The disc is rotated at a calculated speed and temperature that causes the atoms and molecules within the rotator to fuse and precipitate, creating the NPs. The characteristics of the NPs are determined by parameters such as the liquid flow rate, the disc rotation speed, liquid/precursor ratio, and feed and disc surface location.<sup>23</sup> Silver nanoparticles (AgNPs) are a leading example of utilising this technique.<sup>32</sup> The sol-gel method is a well-known technique for synthesising metal oxide NPs.<sup>31</sup> In this method, a liquid precursor (usually metal alkoxides) is transformed into sol and then converted into a network of a structure called gel.<sup>31</sup> Biological synthesis is the most environmentally friendly technique. It is non-toxic and biodegradable. It is considered superior to the methods mentioned above, being more straightforward, cost-effective, and less harmful to the environment and human health.<sup>33</sup> It relies on an enzymatic process that replaces the chemical reactions in the chemical approaches and is not as energy-consuming as the abovementioned techniques.<sup>33</sup> Biosynthesis utilises plants, bacteria, algae and fungi to establish the reaction media and act as a capping agent.<sup>9</sup> This process occurs in three main steps. The selection reaction media, the biological reducing agent and non-carcinogenic substances stabilise the formed nanoparticles.<sup>34,35</sup> Figure 2 demonstrates the use of *Cinnamomum* extract as a stabilising and reducing agent in the biological production of metal nanoparticles. In this example, gold solution was used to create gold nanoparticles (AuNPs). This can be replaced with other metallic solutions to synthesize different types of MNPs.

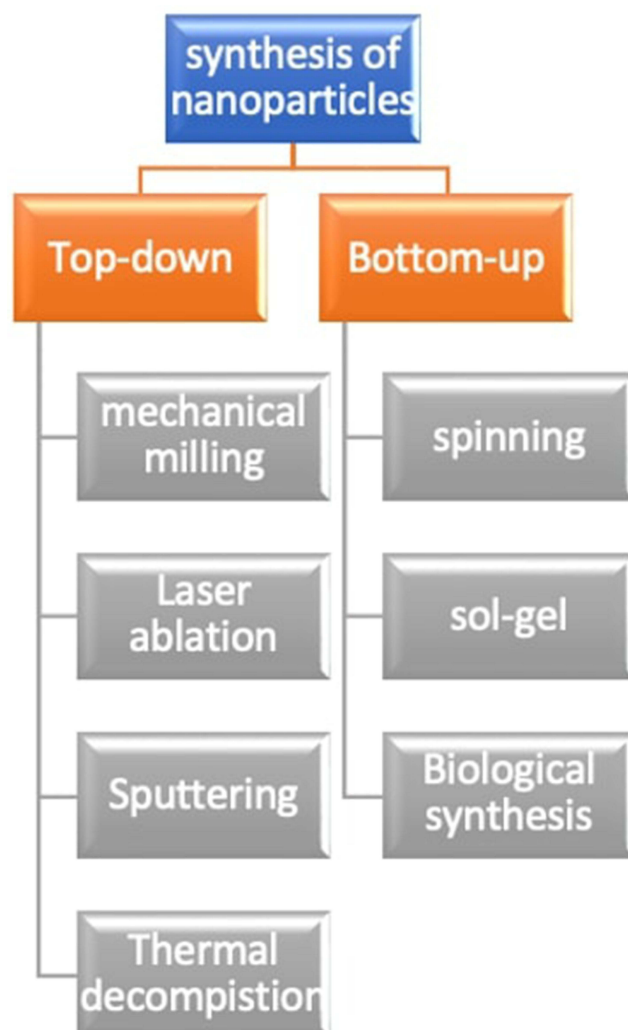


**Figure 1** Diagram illustrating the techniques used in the synthesis of nanoparticles.

## Characterization of Nanoparticles

Nanoparticle parameters like size, shape and surface functionality are essential in determining the application in which the NPs can be utilised. For example, the NPs' size can determine their pathway of entry into the cell, whether phagocytosis or pinocytosis.<sup>36</sup> The shape of the nanoparticle is also essential in determining its functional properties. For example, nanorods with certain aspect ratios were utilised as novel contrast agents to be used in photothermal cancer therapy and molecular imaging.<sup>37,38</sup> The spherical-shaped NPs have an application in the biomedical field, whereas the hexagonal and rectangular-shaped NPs are useful in biomedical imaging.<sup>13</sup> The morphology of the NP can be assessed by microscopical methods, such as scanning electron microscopy (SEM) and transmission electron microscopy (TEM).<sup>39</sup> These techniques will show the size, shape and distribution of the nanoparticles. Spectroscopic techniques such as infrared, ultraviolet-visible (UV), photoluminescence (PL), magnetic resonance and diffuse reflectance spectrometer (DRS) can also reveal the size, shape and concentration of nanoparticles.<sup>39</sup> DRS can show the band gap energy of NPs. PL is used to study the emission and absorption of the incident photons, half-life and the recombining effects of the charges.<sup>39</sup> X-ray diffractometry (XRD) can reveal the phase, particle size, type of the NPs and their crystal nature.<sup>39</sup> Energy-dispersive X-ray spectroscopy (EDX) can determine the elemental composition of the NPs. X-ray photoelectron spectroscopy assesses the composition ratio of the elements that exist in NPs.<sup>39</sup> Raman and Fourier-transform infrared spectroscopy (FTIR) is used to estimate the functional groups involved in the reduction and capping processes. The zeta

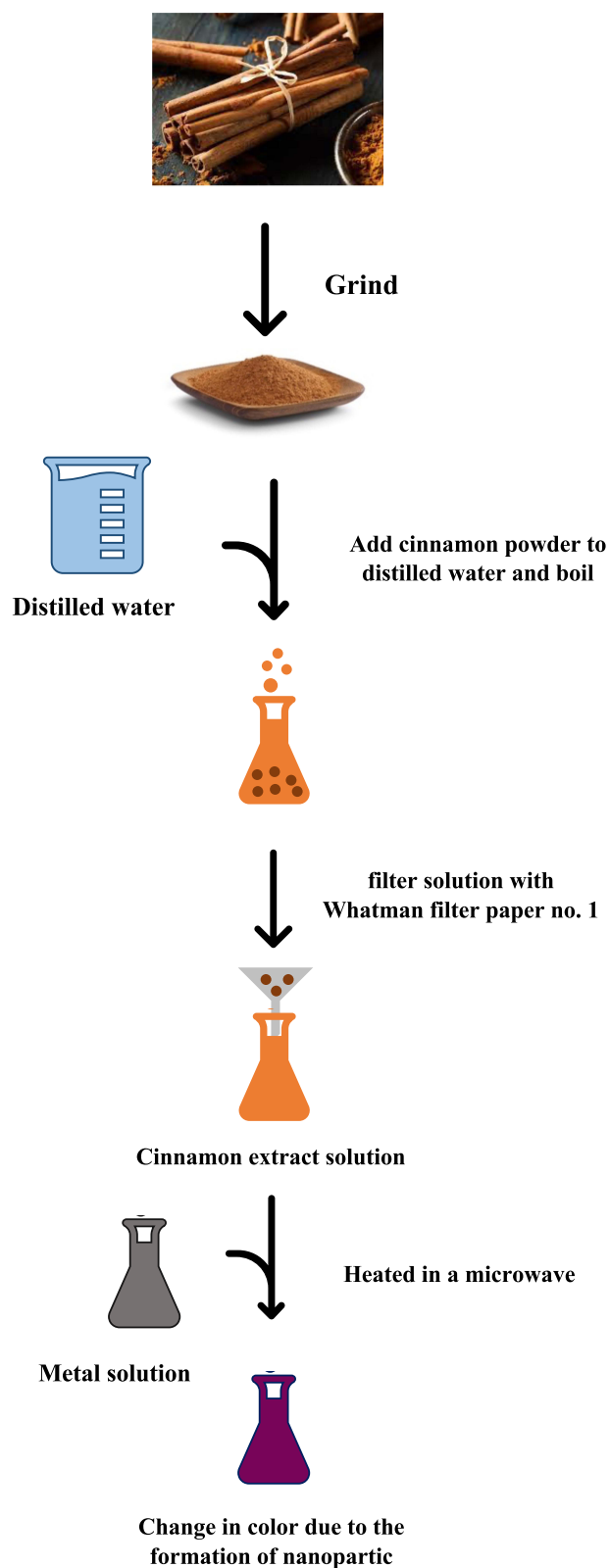


**Figure 2** Steps involved in the biological synthesis of metal nanoparticles using *Cinnamomum* extract as a stabilizing and a reducing agent.

potential is vital to determine the degree of the stability of the NPs by measuring their surface charge potential.<sup>40</sup> Having a large positive or negative zeta potential is an indicator of the excellent physical stability of the NPs.<sup>40</sup>

## Nanoparticles and Their Medical and Biological Applications

MNPs have enormous applications in various interdisciplinary science fields, especially medicine. NPs have been in the nanoscale and have direct access and communications with cells.<sup>41</sup> They can be utilised to construct an excellent drug delivery system. NP-based drug delivery systems in cancer therapy have shown many advantages in terms of pharmacokinetics, precision in targeting tumour cells, reduction in side effects and drug resistance.<sup>42,43</sup> The ability of NPs to circulate throughout the body allows extensive, accurate imaging of different tissues, organs such as the brain, and a comprehensive range of tumours.<sup>44,45</sup> MNPs are believed to have better probe biocompatibility, biodistribution and a longer half-life. These properties facilitate reaching the target with minimal toxicity.<sup>46</sup> Nanoparticles are known to have antimicrobial activity due to their interaction with the microbial intracellular vital components like DNA, RNA and ribosomes, which alter their bioactive processes.<sup>47</sup>

## Cinnamomum

The genus *Cinnamomum* includes different plant species that have long been known for their usage as food, food derivatives and spice.<sup>48</sup> Several traditional healing methods have utilised this plant in herbal medicine to cure various illnesses, such as urinary tract infections, dyspepsia, flatulence, nausea, and as a relief for abdominal discomfort.<sup>48,49</sup> It was confirmed that the bioactive compound of *Cinnamomum* species is intrinsically antimicrobial,<sup>50</sup> antidiabetic,<sup>51</sup> antioxidant,<sup>52</sup> anti-inflammatory,<sup>53</sup> anticancer,<sup>54,55</sup> and neuroprotective.<sup>48</sup> The main bioactive components of *Cinnamomum*, cinnamaldehyde and eugenol, can act as anti-inflammatory substances by inhibiting arachidonic acid's release from the cell membrane.<sup>48</sup> A total of 127 chemical compounds have been identified in the genus *Cinnamomum*.<sup>48</sup> The main compounds identified include cinnamaldehyde, cinnamates, cinnamic acid, and essential oils, mainly containing eugenol. For example, the bark and leaf essential oils of *C. verum* contain eugenol (90.2%) and cinnamaldehyde (44.2%). These components have shown antibacterial effects by inhibiting bacterial beta-lactamase production.<sup>50</sup> The high presence of cinnamaldehyde and eugenol in *Cinnamomum* species grants its vital oxygen and reducing properties, which led many researchers to try and unfold its ability as a bio-reducing agent to produce metal nanoparticles. The *Cinnamomum*'s polyphenols act as capping agents and play a crucial role in controlling the agglomeration of the developed NPs.<sup>13</sup> This process was expected to occur by deprotonating the hydroxyl group of the eugenols in the *Cinnamomum* species.<sup>18</sup> After the deprotonation, the eugenol becomes an anionic form. Electron withdrawing groups in eugenol, such as methoxy and ally group, further oxidize the eugenol, resulting in its strong reduction ability followed by its capping properties.<sup>18</sup> Researchers successfully reported the synthesis of a different variety of MNPs such as silver,<sup>8,11,14,56–60</sup> gold,<sup>17,61–66</sup> copper,<sup>18,67</sup> selenium,<sup>47</sup> manganese,<sup>68</sup> magnetic,<sup>13</sup> zinc oxide<sup>69,70</sup> and titanium oxide.<sup>71</sup> This review discusses the experimental methodology of each of the metal nanoparticles. This is followed by a brief description of their characteristics and their application.

## Cinnamomum-Based Metallic Nanoparticles

### Cinnamomum-Based Silver Nanoparticles

Silver nanoparticles (AgNPs) are known for their application in many fields of science and technology. In the following section, we will briefly describe and discuss the experiments in which *Cinnamomum*-based methods were utilised in the synthesis of AgNPs. For each experiment, we will briefly describe the methodology of *Cinnamomum* extract creation, the analysis of the synthesized nanoparticles and the results of their characterisation. We will also provide the results of their tested application. Table 1 summarises the experiments discussed in this section.

### Synthesis and Characterization

Yadav and Khurana<sup>56</sup> successfully reported the synthesis of AgNPs from aqueous silver nitrate (AgNO<sub>3</sub>) solution utilising *Cinnamomum tamala* leaves Extract as a stabilising and capping agent. Two grams of *C. tamala* leaves were washed, crushed and stirred with 20mL of deionised water for 15–20 mins at 60 °C. The solution was then filtered to be



**Table 1** Summary of the Literature on Greenly Synthesized Silver Nanoparticles Using *Cinnamomum*-Based Extract. Information About the *Cinnamomum* Species Was Utilised, Silver Solution Was Employed, the Average Size of the Synthesized Nanoparticle, Shape, Absorption Peak, Zeta Potential Was Tested, and the Application Was Tested

Author/s	Type of NP Synthesized	<i>Cinnamomum</i> Species	Metal Solution	Average/range of Size of NP	Shape of the Majority of NPs	UV Spectroscopy Absorption Peak	Zeta Potential	Application Tested
Yadav and Kuharana <sup>56</sup>	Silver NPs	<i>C. tamala</i>	Silver nitrate	8 ± 2 nm	Spherical	440 nm	Not reported	Catalyst for the synthesis of pyranopyrazole derivatives
Premkumar et al <sup>11</sup>	Silver NPs	<i>Cinnamon</i>	Silver nitrate	50–70 nm	Spherical	423 nm	Not reported	Antibacterial activity against <i>S. aureus</i> , <i>B. cereus</i> , <i>E. coli</i> and <i>P. aeruginosa</i>
Aref and Salem <sup>58</sup>	Silver NPs	<i>C. camphora</i>	Silver nitrate	5.47 to 9.48	Spherical	420	Not reported	Antibacterial activity against <i>S. aureus</i> , <i>B. subtilis</i> , <i>E. coli</i> and <i>P. aeruginosa</i>
Fatima et al <sup>59</sup>	Silver NPs	<i>C. cassia</i>	Silver nitrate	Average (42 nm), Range (25–55 nm)	Spherical	410	Not reported	Antiviral activity against influenza virus H7N3
Alwan and Al-Saeed <sup>60</sup>	Silver NPs	<i>C. zeylanicum</i>	Silver nitrate	60–80 nm	Shape of the majority of NPs	428	–23.07 mV	Effect on polycystic ovarian syndrome

the cinnamon extract. About 80mL of 0.2mmol/L AgNO<sub>3</sub> was added to 10mL of the *Cinnamomum* extract and was magnetically stirred for 1 hour in a dark room. The colour of the test tube changed from clear transparent to light yellow, then to orange-brown with stirring, indicating the formation of AgNPs. The presence of AgNPs was confirmed using UV-vis spectroscopy with an absorbance peak at 440 nm. The intensity of the peak increased proportionally with the duration of the stirring time, which can be explained by the plasmon resonance phenomena exhibited by the AgNPs. A High-Resolution Transmission Electron Microscopy (HRTEM) image of the sample revealed nanoparticles spherical in shape and ranged from 7–15 nm in size with an average size of 8 ± 2 nm. The AgNP sample was subjected to EDX for elemental analysis and exhibited a strong signal for silver, further confirming the presence of AgNPs.<sup>56</sup> XRD analysis revealed three diffraction peaks, at 38.06°, 44.02°, and 64.36°, which were indexed to the (111), (200), and (220) planes of cubic face-centred silver.<sup>56</sup>

Premkumar et al<sup>11</sup> also reported the successful synthesis of AgNPs from aqueous silver nitrate (AgNO<sub>3</sub>) solution with cinnamon leaf broth as both a reductant and a stabiliser. One-gram cinnamon was obtained from a local store, air dried, ground to powder, placed in 25mL distilled water, and stirred for 25 minutes. The solution was heated for 30 minutes in a water bath at a maintained temperature of 50–60 °C and then filtered. The synthesis of NPs was achieved by adding 10 µL of AgNO<sub>3</sub> to a test tube that contained a ratio of 0.5 mL of cinnamon extract to 4.5 mL of distilled water. The corresponding test tube was kept for 48 hours to be analysed. The colour of the mixture in the test tube changed from transparent yellowish to reddish-brown colour, which suggests the reduction of AgNO<sub>3</sub> to Ag<sup>+</sup> ions. The presence of AgNPs was confirmed using UV-vis spectroscopy. The absorbance peak appeared at 412 nm directly after the 48-hour incubation period and 423.2 nm after being subjected to 3 days of stability testing. The field emission scanning electron microscope (FESEM) revealed monodispersed spherically shaped NPs with sizes ranging from 50 to 70 nm. XRD was utilised to analyse the structural aspect of the AgNPs. XRD of the AgNPs revealed five diffraction peaks at 27.743°, 32.161°, 38.025°, 46.159° and 54.720°, with a corresponding interplanar spacing (d) of 3.21, 2.78, 2.36, 1.96 and 1.67, respectively. FTIR revealed O-H stretch from carboxylic acid, C=N stretch from oxime compound, and C-Cl, C-Br, and C-I stretch from Halo compounds. These compounds are responsible for reducing and capping the Ag<sup>+</sup> ions.<sup>11</sup>

Aref and Salem<sup>58</sup> successfully synthesized AgNPs by utilizing *C. camphora* callus extract. The callus was obtained from a 5–6 week old *C. camphora* plantlets, divided into equal 1g masses and placed in a specialized Murashige and Skoog medium for growth. Each callus was incubated in different light conditions, 1500 lux of white, red, yellow, and blue light. Two grams of dried callus was added to a 100mL of distilled water and heated at 60°C for three hours. The mixture was then filtered using a Whatman filter paper No.1. The filtrate was taken as the callus. Extract (CluE) utilised in the synthesis of AgNPs. One hundred millilitres of the Callus was added to AgNO<sub>3</sub> to reach a final concentration of 1mM.

The mixture was left for 24 hours at a 35°C temperature. The colour of the mixture changed to deep brown, indicating the formation of AgNPs. UV-vis spectroscopy revealed an SPR absorption peak at 420 nm, confirming the formation of the AgNPs. TEM imaging revealed spherical AgNPs that have a homogenous distribution without aggregation. The average size of the NPs was 5.47 to 9.48 nm.<sup>58</sup> EDX confirmed that the major element of the mixture was silver, and the fabrication of AgNPs had a percentage of 57.3%. DLS recorded an average size of AgNPs to be 29.5 nm, which was attributed to the high sensitivity of the DLS, which recorded the size of the substances that are absorbed on the NPs surfaces, such as attached stabilizers, hence giving a higher registered number than the TEM. FTIR analysis of the AgNPs revealed a new band corresponding to binding vibrations of the amide I band protein with N-H stretching. New bands also appeared that correspond to binding OH to the AgNPs. FTIR analysis confirmed that the main component in reducing, stabilizing and capping the AgNPs was the callus extract of *C. camphora*. XRD analysis revealed peaks at 38.3°, 45.52°, 64.44° and 77.54°, with corresponding planes that are indexed at (111), (200), (220) and (311), respectively, which represent planes of silver cubic face-centered (fcc) crystalline form (JCPDS No 87-0720).<sup>58</sup>

Fatima et al<sup>59</sup> successfully synthesized AgNPs using *C. cassia* leaf extract. The *Cinnamomum* bark was obtained and ground. A 25g powder was added to 100 mL of water and then filtered using the Whatman No.1 filter to become the Extract utilised in the experiment. Ten millilitres of the Extract was added to 90 mL of AgNO<sub>3</sub> (1 mM), and the mixture was left at room temperature for 5 hours. The colour changed to dark brown, indicating the silver nanoparticle synthesis. UV-vis spectroscopy revealed a peak at 410 nm. SEM imaging revealed spherical nanoparticles with an average size of 42 nm, and sizes ranged from 25 to 55 nm. FTIR analysis of the AgNPs was compared to the Extract, and minor changes were observed, confirming that the Extract was responsible for reducing the silver ions.<sup>59</sup>

Alwan and Al-Saeed<sup>60</sup> synthesized AgNPs by utilizing *C. zeylanicum* extract. Twenty grams of *C. zeylanicum* powder was added to 100 mL of 80% hydro-methanol (water:methanol, 20:80 v/v). The extract was filtered and dried. Under ultrasound conditions, 5 mL of the extract was added gradually to 200 mL of 1mM AgNO<sub>3</sub>. The mixture was stirred for 20 minutes and stored in a dark room for 72 hours. The colour of the mixture changed to yellow after 20 minutes, reddish brown after 1 hour, brown after 24 hours, and dark brown after 72 hours. The colour change was assumed to be due to the shift in the formation of the AgNPs. The mixtures were then centrifuged at 10,000 rpm for 10 minutes. The precipitate was washed five times to be cleansed from impurities. A UV spectroscopy showed a peak around 428 nm and a small redshift. SEM images showed smooth, spherical particles with different sizes ranging from 60 to 80 nm. FTIR spectrum of the AgNPs showed strong absorption bands corresponding to the hydroxy group (O-H) of phenols and alcohols, carbon hydroxyl (C-H) of alkane, and aldehyde carbonyl (C=O) and (C-H) of alkenes, C-X from alkyl halides and C-N-C from amines. These all confirmed the presence of functional groups in the newly synthesized AgNPs. The AgNPs had an average zeta potential of -23.07 mV. XRD analysis showed diffraction peaks at 2θ values 36.4°, 43.5°, 54.3°, 75.1° for AgNPs, which corresponded to 111, 200, 220 and 311 planes of silver.<sup>60</sup>

## Biological Applications

Yadav and Kuharana<sup>56</sup> assessed their formed AgNPs for their ability as a catalyst in the synthesis of pyranopyrazole derivatives. These compounds are known for their fungicidal, bactericidal and herbicidal properties.<sup>72</sup> When AgNPs were used as catalysts, they yielded 88–92% of pyranopyrazole derivatives. A lower molar concentration of AgNPs led to a lower yield. However, higher molar concentrations did not significantly improve the yield or reaction time. The catalytic role of AgNPs was confirmed by repeating the same reaction without the AgNPs, and the reaction was incomplete after 8 hours and only yielded 25% of the pyranopyrazole derivatives. The AgNPs were then tested for their reusability as catalysts. The recycled NPs effectively yielded pyranopyrazole derivatives for four recycles, after which a drop in yield was observed.<sup>56</sup>

Premkumar et al<sup>11</sup> tested their synthesised AgNPs for antimicrobial activity against *S. aureus*, *B. cereus*, *E. coli* and *P. aeruginosa*. They found the antimicrobial activity increased as the AgNPs concentration increased. The AgNPs were mainly effective against *E. coli* and *P. aeruginosa*. The effect was less robust on *B. cereus* and *S. aureus*.

Aref and Salem<sup>58</sup> assessed their AgNPs antibacterial activity against different gram-positive bacteria (*S. aureus* and *B. subtilis*) and gram-negative bacteria (*E. coli* and *P. aeruginosa*). The AgNPs were more effective against gram-positive than gram-negative. A lower dose of 10 µg/mL exhibited a Minimum inhibitory concentration (MIC) against gram-



positive bacteria equal to a 20 µg/mL AgNPs' MIC against gram-negative bacteria. An inhibition mechanism proposed was through the attachment of the AgNPs to the bacterial membrane that damaged the selective permeability, resulting in a leakage of its cellular constituents. Also, the AgNPs were to inhibit the ATP production required for the vitality of the bacterial cell. Electrostatic attractions between the negative bacterial cell surface and the positive AgNPs charge resulted in cytoplasmic shrinkage, membrane detachment and cell rupture.<sup>58</sup>

Fatima et al<sup>59</sup> tested their AgNPs' for antiviral activity against influenza virus H7N3. Five different concentrations of the *Cinnamomum*-based NPs were used (1, 10, 50, 100, and 200 µg/mL). The *Cinnamomum* antiviral effect was tested as well with five concentrations (31.25, 62.5, 125, 250, and 500 µg/mL). Two exposures were tested, (pre-penetration exposure) and (post-penetration exposure). Pre-penetration exposure is tested when the influenza virus is incubated with *Cinnamomum* and its NPs before it enters the cell. Post-penetration exposure is when the cell is treated with the *Cinnamomum* and its NPs after the virus infects the cell. *Cinnamomum* bark was more efficient as an antiviral in pre-exposure penetration than post-exposure. At higher concentrations of the *Cinnamomum* bark (250, 500 µg/mL), there was no noticeable difference in the antiviral activity. At lower concentrations (31.25, 62.5, and 125 µg/mL), there was significant antiviral activity at pre-exposure penetration. As for the NPs, there was no significant antiviral activity at lower concentrations (1, 10 µg/mL) when the NPs were introduced to the cell after antiviral infection (post-penetration exposure). However, the low concentrations were significantly antiviral when incubated with the NPs before infection (pre-penetration exposure).<sup>59</sup> At higher concentrations (50, 100, and 200 µg/mL), there was statistically significant antiviral activity in both pre-penetration and post-penetration exposures, with higher efficacy in pre-penetration.<sup>59</sup>

Alwan and Al-Saeed<sup>60</sup> assessed their biosynthesized AgNPs using *C. zeylanicum* leaf extract to restore the hormonal imbalance of rats with Estradiol Valerate (EV) induced Polycystic Ovarian Syndrome (PCOS). The serum levels of follicle-stimulating hormone (FSH), Luteinising Hormone (LH), Estradiol (E2), Progesterone (PROG) and testosterone (TEST) levels were assessed in different groups of mice. The hormone levels were assessed in a control group (G1), EV-induced PCOS group (G2), EV-induced PCOS treated with metformin (G3), EV-induced PCOS treated with methanolic bark extract of *C. zeylanicum* (G4) and EV-induced PCOS treated with the biosynthesized AgNPs (G5). The AgNPs were shown to effectively regulate and restore the levels of all of the five hormones contributing to the PCOS.<sup>60</sup> It was also proven that the NPs successfully restored the estrus cycle of the affected mice. It was proposed that the cytotoxic effect of accumulated NPs targeted the polycysts via apoptosis.<sup>60,73,74</sup> Seventy-five percent of the rats in the PCOS were infertile; however, the groups treated with the CZ extract, metformin and AgNPs had a 100% restoration in their fertility rate.<sup>60</sup>

## Cinnamomum-Based Gold Nanoparticles

Gold nanoparticles (AuNPs) have been studied extensively in the medical field due to their lack of harmful response in organisms. Gold particles can be specifically engineered to perform various functions, such as treating malignancies and bacterial infections. The natural inertness of gold, combined with the degree to which it can be engineered into nanoparticles, promises the ability to tailor therapies with fewer side effects.

Furthermore, many naturally occurring and abundant plants can be used in the synthesis process.<sup>75</sup> The synthesis of these gold-based nanoparticles is simple while maintaining a low ecological footprint. The subject of this review, different types of *Cinnamomum* have been studied in the synthesis of AuNPs, such as *Cinnamomum zeylanicum*, *Cinnamomum tamala*, *Cinnamomum cassia*, and *Cinnamomum camphora* were reported to synthesize such particles. The size and shape of the NPs produced are two main points that must be considered during the synthesis process as they determine their properties, such as catalytic productivity as well as their physical, thermal and optical properties.<sup>17,75</sup>

Table 2 summarises the experiments discussed in this section.

## Synthesis and Characterization of Cinnamomum-Based Gold Nanoparticles

Naik et al<sup>17</sup> reported a green synthesis method to develop Au/TiO<sub>2</sub> NPs from *C. tamala* leaves. Similar to *C. zeylanicum*, the solution produced acted as a reductant. This method is accountable for reducing Au<sup>3+</sup> to Au<sup>0</sup>. Naik et al<sup>17</sup> prepared 5g of *C. tamala* leaves, which were finely cut and mixed with 100 mL of distilled water. This mixture was left to boil for 60 minutes at 60 °C. Later, the broth was extracted by filtration after cooling down the boiled mix to room temperature. AuNPs were prepared by mixing 20 mL of distilled water with 1g of P-25 TiO<sub>2</sub> in a beaker and stirring for 30 minutes.

**Table 2** Summary of the Literature on Greenly Synthesized Gold Nanoparticles Using *Cinnamomum*-Based Extract. Information About the *Cinnamomum* Species, Metal Solution Utilised, the Average Size of the Synthesized Nanoparticle, Shape, Absorption Peak, Zeta Potential and the Application Tested are Found Here

Author/s	Type of NP Synthesized	Type of <i>Cinnamomum</i>	Metal Solution	Average/Range of Size of NP	The Shape of Most NPs	UV Spectroscopy Absorption peak	Zeta Potential	Application Tested
Naik et al <sup>17</sup>	Gold NPs	<i>C. tamala</i>	HAuCl <sub>4</sub>	8–20 nm	Spherical	– 500 to 600 nm – 200 to 340 nm for TiO <sub>2</sub>	Not reported	Photocatalytic activity
ElMitwalli et al <sup>63</sup>	Gold NPs	<i>C. bark</i>	HAuCl <sub>4</sub> powder	- Sample A: 35 nm - Sample B: 5 nm - Sample C: 26 nm	Spherical	535 nm	Not reported	Fluorescence activity
Goyal et al <sup>64</sup>	Gold NPs	Cinnamon bark	Hydrogen tetrachloroaurate (III) hydrate (HAuCl <sub>4</sub> ·3H <sub>2</sub> O)	- Spherical: 13 to 20 nm - Spherical anisotropic: 20 nm - Triangular and hexagonal anisotropic: 40 nm	Triangular, hexagonal and spherical	– 522 nm – An additional weak intensity band at 390 nm	Not reported	Antibacterial activity against <i>E. coli</i> and <i>P. aeruginosa</i>
Ling et al <sup>65</sup>	Gold NPs	<i>C. verum</i>	HAuCl <sub>4</sub>	Diameter: 30 nm to 50 nm	Spherical	Peak at 525 nm to 540 nm	Not reported	Effect on Parkinson-like neurodegeneration
Huang et al <sup>66</sup>	Gold NPs	<i>C. camphor</i>	HAuCl <sub>4</sub>	- Nanotriangles: 80 nm - Spherical at 0.5g biomass: 23.4 nm - Spherical at 0.1g biomass: 21.5 nm	Nanotriangle and spherical	– 0.1g of biomass: 570 nm after 2 min then becomes 1000 nm after 60 min – 0.5g of biomass: 570 nm after 2 mins then becomes 530 nm after 60 minutes	Not reported	No application tested

The chloroauric acid (HAuCl<sub>4</sub>) solution of concentration 10–3 M was added by a dropper. The solution was continuously stirred for 4 hours. Next, *C. tamala* extract was added until reduction occurred. Naik et al<sup>17</sup> characterised the Au/TiO<sub>2</sub> NPs produced using XRD, UV-vis diffuse reflectance, FTIR and TEM studies. *C. tamala* leaf extract produced particles that average around 8–20 nm in size and were spherical, which was identified via TEM and FESEM analysis. FESEM analysis indicated the deposition of AuNPs on the surface of TiO<sub>2</sub>. As for XRD studies, there were "no peak shifts of Au/TiO<sub>2</sub> NPs observed, which demonstrates that "the TiO<sub>2</sub> matrix was maintained as the anatase phase".<sup>17</sup> Moreover, DRS UV-vis studies showed that the SPR absorption peak occurred at the spectrum's visible region, indicating the photolytic activity of AuNPs. FTIR analysis also shows peaks of various samples of Au/TiO<sub>2</sub>. This study shows the stretching and bending of various bonds found in Au/TiO<sub>2</sub>.<sup>17</sup>

Elmitwalli et al<sup>63</sup> reported using cinnamon bark extract to synthesize gold nanoparticles and examining its ability to fluorescence quenching of eosin Y dye. The AuNPs are prepared as follows. The cinnamon bark was washed, dried, and ground into a fine powder. A 2.5g of cinnamon bark powder was mixed with 100 mL of double-distilled water, boiled for 5 minutes, and filtered twice. A 1mM of HAuCl<sub>4</sub> solution was prepared. Different volumes of cinnamon extract were added for each 4mL sample of HAuCl<sub>4</sub>. Each sample was then heated in the microwave oven at 1000 W for 15 seconds. A colour change from light yellow to purple-red observed indicates nanoparticle formation.

The NPs produced from Cinnamon were characterised using UV-vis spectroscopy and TEM. The UV-vis analysis showed an SPR absorption peak at 535 nm, indicating the formation of spherical nanoparticles. Absorbance also increases as the amount of cinnamon extract added increases. The shift suggests an increase in size, and the high absorbance indicates they produce more nanoparticles due to a more reducing agent. TEM images show spherical nanoparticles with size. A stock solution of eosin in ethanol was prepared for the quenching. In addition, an albumin stock solution was A with 4mL of eosin stock solution, and sample C was sample B with 50 µL of albumin stock. The AuNPs in sample A had an average size of 35 nm. In sample B, the particles were decreased to 5 nm. Meanwhile, in sample C, the nanoparticles were about 26 nm.<sup>63</sup>

Goyal et al<sup>64</sup> have reported the green synthesis of anisotropic AuNPs with cinnamon bark. The process involves the production of an aqueous cinnamon extract solution that acts as a reducing and stabilizing agent when added to hydrogen tetrachloroaurate (III) due to the presence of trans-cinnamaldehyde in Cinnamon. The solution is formed by immersing 10g of Cinnamon in 100 mL of deionized water for approximately 24 hrs, creating a dark brown mixture, which is then filtered and stored at room temperature. While continuously stirring, this solution is added to 1mM of HAuCl<sub>4</sub>.3H<sub>2</sub>O aqueous solution to synthesize AuNPs. The solution changes from a transparent red wine colour to a red wine, signifying the formation of AuNPs. Goyal et al<sup>64</sup> characterized the nanoparticles produced from Cinnamon using UV-vis spectroscopy, XRD, FTIR and TEM. The UV-vis analysis showed SPR absorption peaks at 522 nm, indicating the formation of spherical nanoparticles.

On the other hand, the two peaks at 390 nm and 540 nm indicate the formation of anisotropic nanoparticles. XRD determined the crystalline phase and size of the nanoparticles. The average crystalline size of spherical NPs was determined to be 14 nm. Furthermore, the size and shape were confirmed by TEM and found to be in the range of 13 nm to 20 nm with an average size of 16 nm. The anisotropic NPs are a mixture of different morphological structures. Spherical anisotropic is 20 nm on average. Triangular and hexagonal anisotropic NPs are 40 nm in size. Additionally, the FTIR study portrayed multiple peaks at 3392, 2121, 1680, 1386, 1227 and 1076 cm<sup>-1</sup>, indicating spherical NPs. Anisotropic NPs had bands at 3323, 2922, 1634, 1432, 1255 and 1075 cm<sup>-1</sup>. Each peak represents a band. It suggests the effects of the phytochemicals found in Cinnamon on reduction and stabilization during AuNPs production.<sup>64</sup>

Ling et al<sup>65</sup> report using *C. verum* to synthesize AuNPs as a treatment for Parkinson's disease (PD) in mice models. They assessed its effects on 1-methyl-4-phenyl-1,2,3,6-tetrahydropyridine (MPTP), which induced PD in mice models. The extract was prepared by adding 24g of *C. verum* leaves to 30 mL of deionized water, and the mixture boiled for approximately 5 minutes. The extract was mixed in 30 mL of HAuCl<sub>4</sub> solution, and the reaction was noted when a change in colour occurred from pale yellow to purple. They further characterized AuNPs through UV-vis spectroscopy and TEM analysis. UV-vis indicated the plasmon peak at 525 to 540 nm. TEM analysis showed that the diameter of most NPs formed ranged between 40 and 50 nm.<sup>65</sup>

Huang et al<sup>66</sup> biosynthesized AuNPs using *C. camphora* leaves. These leaves were turned into a powder form of biomass and mixed with 50 mL of 1mM of HAuCl<sub>4</sub> solution. The solution was mixed at 150 rpm until the reaction was complete.<sup>66</sup> A change in colour from pale yellow to ruby red was observed, indicating the formation of AuNPs. Different amounts of biomass were assessed using UV-Vis, TEM and XDR. A mixture of 0.1g biomass and HAuCl<sub>4</sub> had an SPR peak at 570 nm after 2 minutes of the reaction, a peak at 1000 nm after 60 minutes, and increased intensity.

On the other hand, biomass of 0.5g shows a band at 570 nm after 2 mins and a band at 530 nm after 60 mins. On TEM, it was evident that an increase in the amount of dried powder changed the shape of NPs formed from nanotriangles to spheres. The characterization of the AuNPs on XDR suggested they were crystalline.<sup>66</sup>

### Medical/Biological Application of Cinnamon-based Gold Nanoparticles

Ling et al<sup>65</sup> explore the effects of AuNPs synthesized from *C. verum* on neurodegeneration which was induced in mice models by MPTP to mimic Parkinson's disease (PD). The mice were divided into control, MPTP administered, MPTP with AuNPs (5mg/kg) and MPTP with AuNPs (10mg/kg). Multiple factors were assessed to evaluate the function improvement, including weight, motor impairment, motor function, motor coordination, inflammatory markers, levels of reactive oxygen species (ROS), superoxide dismutase (SOD) activity, myeloperoxidase (MPO) activity, activation of TLR/NF-kB and brain histology. It was revealed that AuNPs prevented weight loss in the mice that were induced with MPTP. Motor impairment was assessed through the pole climbing test. The change was seen as mice that were given MPTP only showed an increase in climbing time compared to the control.

Furthermore, there was a difference between the two doses of AuNPs administered: mice administered with 10mg/kg showed more improvement in pole climbing time than those administered with 5mg/kg. As for motor function, the grasp strength test was used, and it was found that mice treated with MPTP had a stronger grasp due to increased muscle rigidity caused by the compound. AuNPs decrease muscle rigidity, thus decreasing grasp strength to more normal levels. It was observed that 10mg/kg of AuNPs improved motor function by more than 5mg/kg. Additionally, motor coordination was assessed through retention time, which was found through the rota-rod test. MPTP-treated mice had a reduced retention time, indicating negative effects on motor coordination. However, treatment with AuNPs showed increased retention time, indicating recovery.

Ling et al<sup>65</sup> also found many effects of AuNPs administration in mice on immunity. They reported that the compound MPTP caused an increase in the expression of inflammatory markers such as Tumor necrosis factor alpha (TNF-alpha), Interleukin-1 beta (IL-1B) and Interleukin-6 (IL-6). AuNPs decreased the expression of these factors more when a higher dose of AuNPs was administered. In addition, they found an increased production of ROS, a decrease in the activity of SOD and an increase in MPO activity in mice administered with MPTP. However, the administration of AuNPs at higher doses caused a reduction in ROS production, an increase in the activity of SOD and a decrease in MPO activity, respectively.

Ling et al<sup>65</sup> assessed the increase in the activation of Toll-like receptors (TLR) and NF-kB, which are a sign of inflammatory response occurring in the body using the Western blot method. MPTP mostly caused an increase in TLR2, TLR4 and NF-kB. The administration of AuNPs restored the changes induced by the MPTP. As for brain histology, MPTP-induced mice had alterations in the cells present. They had a decrease in the number of neural ganglions, an increase in glial cell lysis and necrotic damage of Purkinje neurons. The administration of a higher dose of AuNPs showed a decrease in changes in the integrity of the normal brain histology. There was less lysis of glial cells as well as less prominent necrotic degeneration of Purkinje neurons.<sup>65</sup>

### Cinnamomum-Based Magnetic Nanoparticles

Magnetic nanoparticles gathered are attractive due to their properties that differ from their bulk materials and their importance in making new devices and materials with new properties.<sup>13,76</sup> They are crucial in making magnetic storage devices, magnetic beads that are used in biotechnology, contrast enhancement in magnetic resonance imaging (MRI), targeted drug delivery and ferrofluids.<sup>13,77</sup> The magnetic nanoparticles that are based on green synthesis have been utilised in semiconductors,<sup>78</sup> catalysts,<sup>13,79</sup> optics<sup>13,80</sup> and medicine.<sup>81</sup>

Iron nanoparticles (FeNPs) gained importance in the industrial sites, textile<sup>82</sup> and plastic industries with coatings made of nanofibre and nanowire.<sup>13</sup> It is also used in tissue repair,<sup>83</sup> drug delivery,<sup>84</sup> biological fluids detoxification,<sup>85,86</sup> hyperthermia,<sup>85</sup> and cell separation by immunoassay.<sup>85</sup> In addition, iron nanoparticles have an antibacterial effect, making them unique from other metal nanoparticles.<sup>87</sup> The magnetic aspect of iron nanoparticles has a beneficial impact on drug delivery to targeted cancer cells.<sup>85</sup> Table 3 summarises the experiment work discussed in this section.

### Synthesis and Characterization

Sivakami et al<sup>13</sup> Successfully synthesized FeNPs using *C. verum* as a reducing and stabilizing agent. *C. verum* barks were washed three times with deionized water. It was then left for three weeks at room temperature to dehydrate. Five grams of *C. verum* were added to 100 mL of distilled water and heated at 70°C for 20 min. It was then left to cool at room temperature. The solution was then filtered by Whatman No.1 paper to be the *Cinnamomum* extract (CES) utilised in the experiment, and the Extract was cooled at 4°C for later use. The CES extract solution was added to 0.01 M of iron chloride (FeCl<sub>3</sub>) by a burette dropwise to obtain a solution in 1:1 proportion with the Extract. The reaction mixture turned black immediately, indicating the reduction of Fe<sup>+</sup> to Fe<sup>0</sup> and the formation of the iron nanoparticles. The reaction mixture was centrifuged at 10,000 rpm for 15 min after 24h. Deionized water and ethanol were used to wash and purify the black pellet formed and left to dehydrate at 60°C in a hot air oven to remove any residual impurities or moisture. The nanoparticle powder was placed in a dry, dark place for further analysis. A UV-vis spectroscopy assessed the newly formed iron nanoparticles, which revealed an SPR peak at 288 nm. XRD analysis suggested that the FeNPs were amorphous as the pattern was deficient at specific diffraction peaks. A characteristic peak of iron NPs was observed at 32.23°. Another peak observed at 22° was attributed to the organic material from the Extract that contributed to the stabilization of the nanoparticles. The average size of the crystallite was 36nm, calculated using Scherer's formula. The XDR analysis was similar to the iron nanoparticles synthesized by Kumar et al<sup>88</sup> using *Terminalia chebula* extract. FTIR analysis revealed peaks that correspond to stretching vibrations of hydroxyl groups (C–H and C–OH) and carbonyl groups (C=O) intimidating aromatic hydrocarbon groups (C=C). The NPs FTIR spectrum showed a slight variation from the original *Cinnamomum verum* extracts. HR-TEM analysis showed circular and spherical-shaped NPs of the iron NPs in detail. Their average size is estimated to be 20–50 nm. No agglomeration of NPs was observed. EDX analysis confirmed the presence of Fe in the NPs. The phytochemical analysis confirmed the presence of Polyphenols, Alkaloids, tannins, Steroids, Terpenoids, and glycosides that contributed to the reduction process. The analysis also revealed a high concentration of antioxidant agents in the *C. verum* bark, which can potentially be exploited in future biomedical applications of the FeNPs.<sup>13</sup>

### Biological Application

Sivakami et al<sup>13</sup> tested their newly synthesized FeNPs' antibacterial activity against *E. coli*, *K. pneumonia*, *S. aureus* and *Bacillus subtilis* by disc diffusion. The diameter of the inhibition zone was 25 mm with *K. pneumonia*, 20 mm with *S. aureus*, 19 mm with *Bacillus subtilis* and 18 mm with *E. coli*. It was concluded that the biosynthesized iron NPs had better antibacterial properties than the standard. It was proposed that reactive oxygen species bound, penetrated and perforated the bacteria's cell membrane, leading to cell wall damage and damaging the interior cell components. The synthesized iron nanoparticles' anti-inflammatory activity was tested and was shown to be more effective than Diclofenac sodium. The iron nanoparticles have also shown a better effect than acarbose when tested for their antidiabetic assay.

### Cinnamomum-Based Copper Nanoparticles

Copper nanoparticles (CuNPs) are cost-effective and have various properties, including thermal and electric conductivity, plasmonic resonance, and photocatalytic behaviour. Its nonmagnetic nature is phenomenal in electronics, electromagnetic interference shielding, metallurgy, heat sinks, military equipment, and medical applications.<sup>18,89</sup> Biosynthesis of CuNPs can be achieved by using different plants and their extracts; however, the weak reductive abilities of plant extracts still prevent their wide usage.<sup>18</sup> In 2020, the importance of CuNPs increased as it was found that the coronavirus has a short maximum time of viability on copper surfaces. Synthesizing stable CuNPs with

**Table 3** Summary of the Literature on Different Types of Metallic Nanoparticles That are Greenly Synthesized Using *Cinnamomum*-Based Extract. Information About the *Cinnamomum* Species Utilised, the Metal Solution Utilised, the Average Size of the Synthesized Nanoparticle, Shape, Absorption Peak, Zeta Potential and the Application Tested are Found Here

Author/s	Type of Nanoparticle Synthesized	<i>Cinnamomum</i> species	Metal Solution	Average/ range of size of NP	Shape of the majority of NPs	UV spectroscopy Absorption peak	Zeta potential	Application tested
Sivakami et al <sup>13</sup>	Magnetic NPs	<i>C. verum</i>	Iron chloride	20–50 nm	Spherical	288 nm	Not reported	Antibacterial activity against <i>S. Aureus</i> and <i>E. coli</i>
Sarwar et al <sup>18</sup>	Copper NPs	<i>C. lauraceae</i>	Copper nitrate	Not reported	Spherical	570–620	Not reported	Catalytic activity
Alghuthaymi et al <sup>47</sup>	Selenium NPs	<i>C. zeylanicum</i>	Sodium selenite	Average (23.3 nm) Range (6.8–58.2 nm)	Spherical	Not reported	–28.6 mV	Antibacterial activity against <i>S. typhimurium</i> , <i>E. coli</i> , <i>S. aureus</i> and <i>L. monocytogenes</i> .
Kamran et al <sup>68</sup>	Manganese NPs	<i>C. verum</i>	Manganese (II) acetate tetrahydrate	50–100 nm	spherical	Not reported	Not reported	Antimicrobial activity against <i>E. coli</i>
Maheswari et al <sup>71</sup>	Titanium oxide NP	<i>C. verum</i>	Titanium dioxide powder	10.5 nm	spherical	UV spectroscopy Absorption peak	Not reported	Anticancer cell activity against oral cancer cell line



disinfectant features on textiles with no toxic reagents can help fight the COVID-19 pandemic.<sup>18,90</sup> Table 3 summarises the experiments discussed in this section.

### Synthesis and Characterization

Sarwar et al<sup>18</sup> successfully synthesized copper oxide nanoparticles (CuONPs) by utilizing *Cinnamomum lauraceae* extract as a reducing and stabilizing agent. *C. lauraceae* leaves were obtained from the local store, washed with distilled water, let dry, and ground into a fine powder.<sup>18</sup> Ten grams of the ground powder were added to a 100 mL water flask and boiled for 40 minutes. The solution was then double-filtered using Whatman filter paper No.1 to become the *Cinnamomum* extract (CES) utilised in the experiment. Three millilitres of the CES and 30 mL of 0.1 mM copper nitrate were added to a glass beaker. The solution mixture was divided into three samples (10 mL each), and the pH was set to 3.7 and 11, respectively, using ammonia water. The samples were then heated at 90°C with continuous stirring at 700 RPM and observed visually for any colour change. The samples were assessed by UV-Vis spectroscopy and revealed a maximum absorption peak at 570–620 nm of wavelength. Furthermore, to find the optimum volume of CES to produce copper NPs, different amounts (1,2,3,4 and 5 mL) of the CES were added to 0.1 mM copper salt solution (keeping to 10mL total volume) using the optimized pH 11. UV-visible absorption spectrum was then used to assess the solutions and the optimized CES quantity was determined to be 4 mL as it had the highest absorption and the most distinct peak. Different concentrations of citric acid were added to the reaction medium (with 4mL of CES, pH11) with 1–5% of the total volume. The UV-Vis spectrum showed sharp peaks, and the amount of citric acid increased until the solution acquired the standard brick-red colour of CuONPs. Field emission scanning electron microscopy (FESEM) was used to examine the surface morphology of the CuONPs. FESEM showed a uniform spherical shape, and the texture of the surface was consistent. At the same time, the CuONPs without citric acid had a non-uniform shape and an uneven hirsute surface texture. The EDX spectrum showed retention of the most substantial copper peaks at 1.00 KeV and 8.00 KeV, which supports the presence of the copper with 84.77% weight composition.<sup>18</sup> XRD analysis reveals strong peaks at 43.4°, 50.6°, and 74.2°, which corresponded to the (111), (200) and (220) planes of copper, respectively, with a slight deviation from the standard JCPDS. No. 01–085-1326 of copper. This slight deviation is due to surface capping and particle size distribution while the small peak at 39.05° might be due to slight surface oxidation. FTIR spectroscopy revealed strong bands corresponding to vibrations of the -C-O of primary alcohols in eugenol and -OH, -C=O and -C=C groups present in the Extract's metabolites confirmed to be responsible for the capping of the NPs after their synthesis. The presence of citric acid indicated better capping by showing a sharper peak for -C=O and -C=C.

### Biological Application

Sarwar et al<sup>18</sup> tested the antimicrobial activity of the biosynthesized CuONPs (with and without mediation with citric acid) with *S. Aureus* and *E. Coli* bacterium using disc diffusion. The control sample had no inhibition zone, while CuONP samples, with and without mediation with citric acid, were shown to be effective against the bacteria mentioned above. However, citric acid-mediated CuNPs showed better antibacterial activity with their larger inhibition zone. The improved activity is due to an increased surface/volume ratio when citric acid is added. Citric acid also has antimicrobial activity, which was proposed to have caused a higher antibacterial effect. Sarwar et al<sup>18</sup> also reported the effectiveness of their NPs in degrading dyes in a non-toxic technique.

### Cinnamomum-Based Selenium Nanoparticles

Selenium nanoparticles (SeNPs) are known to have low toxicity and high biocompatibility, making them the centre of research for their application in therapeutics and theragnostic agents.<sup>91</sup> SeNPs are also known for their antimicrobial and antiviral activity.<sup>92,93</sup> SeNPs can be utilised in encapsulated drugs or carriers to reach and kill cancer cells.<sup>94</sup> SeNPs can also suppress cancer growth by acting as immunomodulatory agents, acting on the tumor-associated macrophages and sending activation signals to specific T cells.<sup>95,96</sup> SeNPs are known to have anti-oxidative and anti-inflammatory activity, allowing them to be applied to medical disorders such as arthritis, diabetes and nephropathy.<sup>97</sup> SeNPs can control the production of cytokines to activate innate immunity, eventually exhibiting antimicrobial activity.<sup>98</sup> Table 3 summarises the experiments discussed in this section.

## Synthesis and Characterization

Alghuthaymi et al<sup>47</sup> successfully photosynthesized SeNPs using *Cinnamomum zeylanicum* as a reducing agent. In the experiment, *C. zeylanicum* barks were obtained, powdered, and immersed in 10-fold (w/v) from 70% ethanol for a period of 15 hours. The extract solution was then filtered out of the bark residues. A 10 mm of sodium selenite ( $\text{Na}_2\text{SeO}_3$ ) was prepared and added to equal volumes of CIE aqua solutions to have a total concentration of 0.5%, 1.0%, and 1.5%. The solutions were stirred for 6 hours at a 25°C temperature. The colour of the solutions changed to brownish orange, indicating the formation of SeNPs. The optimal concentration of the CE aqua solution for synthesising SeNPs was 1%, as observed from the colour deepness.<sup>47</sup> The SeNPs were characterized by TEM, which revealed the presence of spherically shaped NPs with no aggregation. The size range of the NPs was 6.8 to 58.2 nm, with an average mean diameter of 23.3 nm. Little CIE particles were also observed in combination with the synthesized SeNPs, the same was observed in other research papers.<sup>99</sup> FTIR assessment of the synthesized SeNPs to identify the biomolecules responsible for reducing and capping the selenium ions. The observed peaks were denoted to carbonyl groups and another O-H stretching group of alcohols and phenols. The involvement of the C=O bond in the cinnamon aldehyde in the SeNP was also observed in the FTIR. The zeta potential of SeNPs was -28.6 mV, indicating stable NPs.

## Biological Applications

Alghuthaymi et al<sup>47</sup> studied the antibacterial activity of the synthesized SeNPs against *S. typhimurium*, *E. coli*, *S. aureus* and *L. monocytogenes*. The highest sensitivity to SeNPs was *S. typhimurium*. The effects of SeNPs on *S. typhimurium* and *E. coli* were analysed by SEM at 0, 5 and 10 hours of exposure. At 0 hours, healthy, normal, smooth bacteria and contracted cell walls were observed. This sample served as the control. After 5 hours of exposure, apparent morphological changes were observed; a puffy bacterial cell wall appearance was observed, with many NPs entering the bacterial cell after attaching to and disturbing its cell membrane. Many other bacterial cells were lysed at 5 hours, and the general viability of the remaining bacterial cells decreased. At 10 hours, almost all bacterial cells were lysed. It was proposed that the smaller the size of the SeNPs and their spherical shape, the higher their antibacterial activity since a higher concentration of SeNPs can infiltrate the bacterial cell wall and halt its biological activities. SeNPs exhibit inhibitory activity against gram + bacteria, including *Proteus sp* and *Serratia sp*, which was attributed to lesser surface charges of the SeNPs.<sup>47,100</sup> TEM and SEM imaging of *S. aureus* treated with SeNP have shown their cells shrank, deformed and damaged.<sup>47,101</sup> The exact mechanism by which SeNP act as an antimicrobial is still unknown.

## Cinnamomum-Based Manganese Nanoparticles

### Synthesis and Characterization

Kamran et al<sup>68</sup> successfully synthesized Manganese nanoparticles (MnNPs) using *C. verum* bark as a capping and a reducing agent. Dried *C. verum* bark was ground and sieved in a 300 mm size sieve. Ten grams of the powder was added to 500 mL of distilled water. The mixture was heated at 70°C, stirred continuously for two hours and used as an extract in the experiment. Twelve grams of manganese (II) acetate tetrahydrate [ $\text{Mn}(\text{CH}_3\text{CO}_2)_2$ ] was added to 9g of sodium alginate ( $\text{C}_6\text{H}_9\text{NaO}_7$ ) and 8g of *C. verum* powder, and the mixture was stirred until homogenous solution was achieved. Four hundred millilitres of the Extract was added to the homogenous mixtures and was sonicated at 60°C for 7 hs. A colour change was observed from light brown to dark brown. The mixture was centrifuged at 4000 rpm for 15 min. The sample was then washed with distilled water and methanol and dried in an oven at 70°C for 3 hs. SEM images confirmed the presence of spherical NPs with different sizes and a tendency to aggregate. TEM imaging determined the size range of 50 to 100 nm. XRD analysis revealed the peaks 28.33°, 40.53° and 50.01° at 2 $\theta$  that are indexed as face-centred cubic. FTIR analysis of the synthesized MNPs after dye degradation revealed peaks indicating stretching vibration of a hydroxyl group, C-O bond and an Mn-O bond. Table 3 summarises the experiments discussed in this section.

## Biological Applications

Kamran et al<sup>68</sup> tested the antimicrobial activity of their MNPs. Significant antimicrobial activity was recorded. For *E. coli*, the zones of inhibition were  $16 \pm 0.5$ ,  $18 \pm 0.6$ ,  $20 \pm 0.45$  and  $22 \pm 0.25$  (mm) at 0.4, 0.6, 0.8 and 1mg/mL of

MnNP concentrations, respectively. For *S. aureus*, the zones of inhibition were  $18 \pm 0.7$ ,  $20 \pm 0.35$ ,  $23 \pm 0.25$  and  $24.5 \pm 0.55$  (mm) for 0.4, 0.6, 0.8 and 1 mg/mL of MnNP concentrations, respectively. MnNPs had zones of inhibition comparable to Streptomycin (standard antibiotic).

## Cinnamomum-Based Titanium Dioxide Nanoparticles

Titanium oxide NPs ( $\text{TiO}_2$ NPs) have been in the spotlight of research due to their unique exhibit of excellent antibacterial and anticancer properties.<sup>102,103</sup> These properties were mainly mediated by ROS.<sup>102,103</sup>  $\text{TiO}_2$ NPs are also known for their excellent photocatalytic activity.<sup>104</sup> Table 3 summarises the experiments discussed in this section.

### Synthesis and Characteristics

Maheswari et al<sup>71</sup> successfully reported the synthesis of  $\text{TiO}_2$ NPs using *C. verum* extract. The *Cinnamomum* was washed with deionised water three times, and then 10g of *C. verum* was crushed and mixed with 100 mL of deionised water and heated for 30 minutes at 60°C. The solution was then filtered using a Whatman filter and stored at 4 °C for further use. Twenty millilitres of deionised water was mixed with 0.2 g Titanium dioxide powder, then 4 mL of Cinnamon extract was added to the mixture and stirred at room temperature for two hours, then centrifuged and dried in the oven at 100°C. The solution was assessed by UV spectroscopy and revealed an SPR absorption peak at 330 nm, which was slightly red-shifted than the pure  $\text{TiO}_2$  due to the chemisorption of Cinnamon molecules on the surface of  $\text{TiO}_2$ . TEM and HRTEM analysis showed the  $\text{TiO}_2$ NPs to be spherical and have an average particle size of 10.5 nm. The presence of biomolecules and changes in pH and ionic strength can disturb the delicate balance and allow NPs to form large aggregates in such complex biological fluids. HRTEM images showed crystalline fringes, indicating the great crystalline nature of the  $\text{TiO}_2$  samples. XRD analysis revealed peaks at 25.3°, 37.8°, 48°, 54.7°, 63°, 7° w with corresponding planes that are indexed at (101), (004), (200), (105), (204), (220) and (215), respectively, which is constant with JCPDS file No: 21–1272 of anatase  $\text{TiO}_2$ . FTIR spectroscopy showed peaks corresponding to cineole and cinnamaldehyde (the main components of Cinnamon). A slight variation between the peak of the  $\text{TiO}_2$ NPs and the Cinnamon confirmed a reaction between them.

### Biological Applications

Maheswari et al<sup>71</sup> measured the anticancer effect using five different concentrations of  $\text{TiO}_2$ NPs against the KB oral cancer cell line. It was noted that the Cinnamon modified  $\text{TiO}_2$ NPs had much better anticancerous activities when compared to the pure sample. As the concentration of the NPs increased, the anticancer activity increased. This was attributed to the increased number of NPs penetrating the cells, producing more superoxide radicals, which damage the cancer cells.<sup>71,105</sup> The cinnamaldehyde in Cinnamon is also proposed to cause cancer cell damage.<sup>71,106</sup> The antibacterial properties of the pure and Cinnamon modified  $\text{TiO}_2$ NPs were tested using the zone of inhibition method against Gram-positive and Gram-negative bacteria.<sup>71</sup> The *Cinnamomum* modified  $\text{TiO}_2$ NPs showed no antibacterial activity against any bacterial strain, but the pure  $\text{TiO}_2$ NPs had some antibacterial activity against Gram-positive bacteria.<sup>71</sup>

## Discussion of Literature Review Findings

The synthesis of MNPs can be achieved through various approaches, many of which involve chemical and physical methods that are costly and environmentally hazardous. Green synthesis methods, in contrast, are eco-friendly, cost-effective, and straightforward. Among these, *Cinnamomum*-based synthesis has emerged as a particularly effective and reliable method. The reviewed studies primarily focus on silver nanoparticles (AgNPs), followed by gold nanoparticles (AuNPs), and, to a lesser extent, other metallic nanoparticles such as copper, selenium, manganese, and titanium oxide.

With regard to the reported nanoparticle size, AgNP sizes ranged broadly from 5.47 nm to 80 nm, indicating a dependence on synthesis parameters like extract concentration, reaction temperature, and metal precursor concentration. AgNP shapes are predominantly spherical, suggesting uniformity in the reduction process with *Cinnamomum* extracts. AuNP shapes exhibit greater variety, including spherical, triangular, and hexagonal, with sizes ranging from 5 nm to 80 nm. Other metallic nanoparticles consistently demonstrate spherical shapes, with size ranges reflecting synthesis optimization for specific applications.

AgNPs demonstrate UV-Vis absorption peaks primarily between 410 nm and 440 nm, consistent with their surface plasmon resonance (SPR) characteristics. AuNPs show broader peaks, ranging from 500 nm to 600 nm, corresponding to variations in size and shape. Peaks outside these ranges, particularly in studies involving anisotropic shapes, reflect the role of *Cinnamomum* extracts in modulating nanoparticle morphology. Zeta potential is reported inconsistently across studies. When mentioned (eg,  $-23.07$  mV for silver and  $-28.6$  mV for selenium nanoparticles), it indicates good stability due to the electrostatic repulsion between particles. This reflects the dual role of *Cinnamomum* extracts as both reducing and capping agents.

## Health Aspects of Green Synthesis of Metal Nanoparticles Using *Cinnamomum*-Based Extract

The majority of studies demonstrate antibacterial activity against pathogens such as *E. coli*, *S. aureus*, *P. aeruginosa*, and *B. subtilis*, underscoring the potential for antimicrobial treatments. AgNPs are highly effective against gram-positive bacteria and have shown potential in restoring hormone levels and fertility in PCOS-induced mice.<sup>58–60</sup> AuNPs show promise in treating Parkinson's disease by improving motor function, motor coordination and decreasing muscle rigidity in mice with neurodegeneration.<sup>65</sup> It has also shown anti-inflammatory activities by reducing inflammatory markers such as TNF-alpha, IL-1B and IL-6.<sup>65</sup> Iron NPs exhibited excellent antibacterial properties, stronger anti-inflammatory activities than Diclofenac sodium and better antidiabetic effects than acarbose<sup>13</sup>. Copper, selenium, and manganese NPs exhibit strong antimicrobial effects, particularly against gram-positive bacteria.<sup>18,47,68</sup> Lastly, titanium nanoparticles showed anticancer activity against KB oral cancer cells and antibacterial properties.<sup>71</sup>

## Limitations of This Literature Review

This study faced several limitations. First, access restrictions to many original articles and reports due to paywalls limited the inclusion of potentially valuable studies. Another significant limitation was the variation in methodologies across the reviewed studies, as differences in extraction techniques, solvent choices, metal precursors, and synthesis conditions hindered direct comparisons and the ability to establish standardized conclusions. Furthermore, inconsistencies in nanoparticle characterization techniques, with different studies employing different methods such as SEM, TEM, XRD, and FTIR led to challenges in correlating synthesis methods with nanoparticle properties. Lastly, while the literature review explored the potential applications of *Cinnamomum*-derived nanoparticles, there is a lack of comprehensive toxicological data and an emphasis on laboratory-scale synthesis, with a notable gap in understanding the nanoparticles' cytotoxicity and environmental impact. Without rigorous toxicological evaluations, the potential risks associated with the use of these nanoparticles remain unclear.

## Conclusion

The synthesis of metal nanoparticles using *Cinnamomum*-based extracts provides an eco-friendly, cost-effective alternative to conventional chemical and physical methods. These extracts serve as natural reducing, capping, and stabilizing agents, enabling the formation of nanoparticles with properties comparable to those produced by traditional methods. The literature primarily focuses on silver and gold nanoparticles, with other metals like copper, selenium, manganese, and titanium oxide explored to a lesser extent.

*Cinnamomum* extracts are versatile agents capable of synthesizing nanoparticles with applications ranging from antimicrobial to catalytic and disease-specific treatments. While the spherical shape of nanoparticles indicates reliable stabilization, variations in size and UV-Vis absorption peaks suggest opportunities for further optimization. However, the lack of uniform zeta potential reporting and comprehensive toxicological profiles highlights the need for standardized methodologies and rigorous safety evaluations.

Furthermore, these nanoparticles exhibit a wide range of biological and medical applications, including antifungal, antiviral, and antibacterial activities, as well as therapeutic potential against diabetes, PCOS, and cancer. This review serves as a practical guide for researchers and practitioners interested in accessible, sustainable methods for synthesizing MNPs.

## Abbreviation

AgNPs, Silver nanoparticles; AuNPs, Gold nanoparticles; CuNPs, Copper nanoparticles; CuONPs, Copper oxide nanoparticles; DRS, Diffuse reflectance spectrometer; EDX, Energy-dispersive X-ray spectroscopy; FeNPs, Iron nanoparticles; FESEM, Field emission scanning electron microscopy; FTIR, Fourier-transform infrared spectroscopy; HAuCl<sub>4</sub>, chloroauric acid; IL-1B, Interleukin-1 beta; IL-6, Interleukin-6; LSPR, Localised surface plasmon resonance; MnNPs, Manganese nanoparticles; MNPs, Metal nanoparticles; MPTP, 1-methyl-4-phenyl-1,2,3,6-tetrahydropyridine; MPO, myeloperoxidase; MRI, Magnetic resonance imaging; NP, Nanoparticle; PL, Photoluminescence; ROS, reactive oxygen species; SEM, Scanning electron microscopy; SeNPs, Selenium nanoparticles; SOD, superoxide dismutase; TEM, Transmission electron microscopy; TiO<sub>2</sub>NPs, Titanium oxide NPs; TNF-alpha, Tumor necrosis factor alpha; TLR, Toll-like receptor; UV, Ultraviolet-visible; XRD, X-ray diffractometry.

## Disclosure

The authors declare no conflicts of interest regarding the publication of this paper. The abstract of this paper was presented at the RCSI Annual Research Conference 2023 as a poster presentation with interim findings. The poster's abstract was not published anywhere.

## References

1. Rafique M, Sadaf I, Rafique MS, Tahir MB. A review on green synthesis of silver nanoparticles and their applications. *Artif Cells Nanomed Biotechnol.* **2017**;45(7):1272–1291. doi:10.1080/21691401.2016.1241792
2. Zhang D, Ma XL, Gu Y, Huang H, Zhang GW. Green synthesis of metallic nanoparticles and their potential applications to treat cancer. *Front Chem.* **2020**;8:799. doi:10.3389/fchem.2020.00799
3. Saini R, Saini S, Sharma S. Nanotechnology: the future medicine. *J Cutan Aesthet Surg.* **2010**;3(1):32–33. doi:10.4103/0974-2077.63301
4. Tang S, Mao C, Liu Y, Kelly DQ, Banerjee SK. Protein-mediated nanocrystal assembly for flash memory fabrication. *IEEE Trans Electron Devices.* **2007**;54(3):433–438. doi:10.1109/TED.2006.890234
5. Thakkar KN, Mhatre SS, Parikh RY. Biological synthesis of metallic nanoparticles. *Nanomedicine.* **2010**;6(2):257–262. doi:10.1016/j.nano.2009.07.002
6. Duan H, Wang D, Li Y. Green chemistry for nanoparticle synthesis. 10.1039/C4CS00363B. *Chem Soc Rev* **2015**;44(16):5778–5792. doi:10.1039/C4CS00363B
7. Ijaz I, Gilani E, Nazir A, Bukhari A. Detail review on chemical, physical and green synthesis, classification, characterizations and applications of nanoparticles. *Green Chem Lett Rev.* **2020**;13(3):223–245. doi:10.1080/17518253.2020.1802517
8. Sathishkumar M, Sneha K, Won SW, Cho CW, Kim S, Yun YS. Cinnamon zeylanicum bark extract and powder mediated green synthesis of nano-crystalline silver particles and its bactericidal activity. *Colloids Surf B Biointerfaces.* **2009**;73(2):332–338. doi:10.1016/j.colsurfb.2009.06.005
9. Akhtar MS, Panwar J, Yun Y-S. Biogenic synthesis of metallic nanoparticles by plant extracts. *ACS Sustainable Chem. Eng.* **2013**;1(6):591–602. doi:10.1021/sc300118u
10. Sharma D, Kanchi S, Bisetty K. Biogenic synthesis of nanoparticles: a review. *Arabian J Chem.* **2019**;12(8):3576–3600. doi:10.1016/j.arabjc.2015.11.002
11. Premkumar J, Sudhakar T, Dhakal A, Shrestha JB, Krishnakumar S, Balashanmugam P. Synthesis of silver nanoparticles (AgNPs) from cinnamon against bacterial pathogens. *Biocatal Agric Biotechnol.* **2018**;15:311–316. doi:10.1016/j.bcab.2018.06.005
12. Muhammad DRA, Dewettinck K. Cinnamon and its derivatives as potential ingredient in functional food—A review. *Int J Food Prop.* **2017**;20(sup2):2237–2263. doi:10.1080/10942912.2017.1369102
13. Sivakami M, Renuka R, Thilagavathi T. Green synthesis of magnetic nanoparticles via *Cinnamomum verum* bark extract for biological application. *J Environ Chem Eng.* **2020**;8(5):104420. doi:10.1016/j.jece.2020.104420
14. Li W, Qu F, Chen Y, et al. Antimicrobial activity of silver nanoparticles synthesized by the leaf extract of *Cinnamomum camphora*. *Biochem Eng J* **2021**;172:108050. doi:10.1016/j.bej.2021.108050
15. Unlu M, Ergene E, Unlu GV, Zeytinoglu HS, Vural N. Composition, antimicrobial activity and in vitro cytotoxicity of essential oil from *Cinnamomum zeylanicum* Blume (Lauraceae). *Food Chem Toxicol.* **2010**;48(11):3274–3280. doi:10.1016/j.fct.2010.09.001
16. Lin CT, Chen CJ, Lin TY, Tung JC, Wang SY. Anti-inflammation activity of fruit essential oil from *Cinnamomum insularimontanum* Hayata. *Bioresour Technol.* **2008**;99(18):8783–8787. doi:10.1016/j.biortech.2008.04.041
17. Naik GK, Mishra PM, Parida K. Green synthesis of Au/TiO<sub>2</sub> for effective dye degradation in aqueous system. *Chem Eng J.* **2013**;229:492–497. doi:10.1016/j.cej.2013.06.053
18. Sarwar N, Humayoun UB, Kumar M, et al. Citric acid mediated green synthesis of copper nanoparticles using cinnamon bark extract and its multifaceted applications. *J Cleaner Prod.* **2021**;292:125974. doi:10.1016/j.jclepro.2021.125974
19. Murthy SK. Nanoparticles in modern medicine: state of the art and future challenges. *Int J Nanomed.* **2007**;2(2):129–141.
20. Khan I, Saeed K, Khan I. Nanoparticles: properties, applications and toxicities. *Arabian J Chem.* **2019**;12(7):908–931. doi:10.1016/j.arabjc.2017.05.011
21. Vaidya S, Ganguli AK. 2.01 - Microemulsion Methods For Synthesis Of Nanostructured Materials☆. In: Andrews DL, Lipson RH, Nann T, editors. *Comprehensive Nanoscience and Nanotechnology (Second Edition)*. Academic Press; **2019**:1–12.
22. Talapin DV, Shevchenko EV. Introduction: nanoparticle chemistry. *Chem Rev.* **2016**;116(18):10343–10345. doi:10.1021/acs.chemrev.6b00566



23. Anu Mary Ealia S, Saravanakumar MP. A review on the classification, characterisation, synthesis of nanoparticles and their application. *IOP Conf Ser Mater Sci Eng.* **2017**;263:032019. doi:10.1088/1757-899x/263/3/032019
24. Hu X, Zhang Y, Ding T, Liu J, Zhao H. Multifunctional gold nanoparticles: a novel nanomaterial for various medical applications and biological activities. Review. *Front Bioeng Biotechnol.* **2020**;8(990). doi:10.3389/fbioe.2020.00990
25. Odularu AT. Metal nanoparticles: thermal decomposition, biomedical applications to cancer treatment, and future perspectives. *Bioinorg Chem Appl.* **2018**;2018:9354708. doi:10.1155/2018/9354708
26. Prasad Yadav T, Manohar Yadav R, Pratap Singh D. Mechanical milling: a top down approach for the synthesis of nanomaterials and nanocomposites. *Nanosci Nanotechnol.* **2012**;2(3):22–48. doi:10.5923/j.nn.20120203.01
27. Arbain R, Othman M, Palaniandy S. Preparation of iron oxide nanoparticles by mechanical milling. *Miner Eng.* **2011**;24(1):1–9. doi:10.1016/j.mineng.2010.08.025
28. Shojaei M, Shokuhfar A, Zolriasatein A. Synthesis and characterization of CuAlS<sub>2</sub> nanoparticles by mechanical milling. *Mater Today Commun.* **2021**;27:102243. doi:10.1016/j.mtcomm.2021.102243
29. Bokhonov BB, Dudina DV. Synthesis of ZrC and HfC nanoparticles encapsulated in graphitic shells from mechanically milled Zr-C and Hf-C powder mixtures. *Ceram Int* **2017**;43(16):14529–14532. doi:10.1016/j.ceramint.2017.07.164
30. Cele T. Preparation of Nanoparticles. **2020**.
31. Baig N, Kammakakam I, Falath W. Nanomaterials: a review of synthesis methods, properties, recent progress, and challenges. 10.1039/D0MA00807A. *Mater Adv.* **2021**;2(6):1821–1871. doi:10.1039/D0MA00807A
32. Tai CY, Wang Y-H, Tai C-T, Liu H-S. Preparation of silver nanoparticles using a spinning disk reactor in a continuous mode. *Ind Eng Chem Res.* **2009**;48(22):10104–10109. doi:10.1021/ie9005645
33. Li X, Xu H, Chen Z-S, Chen G. Biosynthesis of nanoparticles by microorganisms and their applications. *J Nanomater.* **2011**;2011:270974. doi:10.1155/2011/270974
34. El-Shishtawy RM, Asiri AM, Al-Otaibi MM. Synthesis and spectroscopic studies of stable aqueous dispersion of silver nanoparticles. *Spectrochimica Acta Part A.* **2011**;79(5):1505–1510. doi:10.1016/j.saa.2011.05.007
35. Keat CL, Aziz A, Eid AM, Elmarzugi NA. Biosynthesis of nanoparticles and silver nanoparticles. *Bioresources Bioprocess.* **2015**;2(1):47. doi:10.1186/s40643-015-0076-2
36. Barar J. Bioimpacts of nanoparticle size: why it matters? *Bioimpacts.* **2015**;5(3):113–115. doi:10.1517/bi.2015.23
37. Liu Y, Tan J, Thomas A, Ou-Yang D, Muzykantov VR. The shape of things to come: importance of design in nanotechnology for drug delivery. *Ther Deliv.* **2012**;3(2):181–194. doi:10.4155/tde.11.156
38. Huang X, El-Sayed IH, Qian W, El-Sayed MA. Cancer cell imaging and photothermal therapy in the near-infrared region by using gold nanorods. *J Am Chem Soc.* **2006**;128(6):2115–2120. doi:10.1021/ja057254a
39. Nkele AC, Ezema FI, Nkele AC. Diverse synthesis and characterization techniques of nanoparticles. *RSC Advances.* **2020**;10:13139–13148. doi:10.1039/d0ra01532f
40. Joseph E, Singhvi G. Chapter 4 - Multifunctional nanocrystals for cancer therapy: a potential nanocarrier. In: Grumezescu AM, editor. *Nanomaterials for Drug Delivery and Therapy*. William Andrew Publishing; **2019**:91–116.
41. Mody VV, Siwale R, Singh A, Mody HR. Introduction to metallic nanoparticles. *J Pharm Bioallied Sci.* **2010**;2(4):282–289. doi:10.4103/0975-7406.72127
42. Yao Y, Zhou Y, Liu L, et al. Nanoparticle-based drug delivery in cancer therapy and its role in overcoming drug resistance. *Rev Front mol Biosci.* **2020**;7. doi:10.3389/fmolb.2020.00193
43. Dadwal A, Baldi A, Kumar Narang R. Nanoparticles as carriers for drug delivery in cancer. *Artif Cells Nanomed Biotechnol.* **2018**;46(sup2):295–305. doi:10.1080/21691401.2018.1457039
44. Nune SK, Gunda P, Thallapally PK, Lin -Y-Y, Forrest ML, Berkland CJ. Nanoparticles for biomedical imaging. *Expert Opin Drug Delivery.* **2009**;6(11):1175–1194. doi:10.1517/17425240903229031
45. Masserini M. Nanoparticles for brain drug delivery. *ISRN Biochem.* **2013**;2013:238428. doi:10.1155/2013/238428
46. Forte E, Fiorenza D, Torino E, et al. Radiolabeled PET/MRI nanoparticles for tumor imaging. *J Clin Med.* **2019**;9(1):89. doi:10.3390/jcm9010089
47. Alghuthaymi MA, Diab AM, Elzahy AF, Mazrou KE, Tayel AA, Moussa SH. Green biosynthesized selenium nanoparticles by cinnamon extract and their antimicrobial activity and application as edible coatings with nano-chitosan. *J Food Qual.* **2021**;6670709. doi:10.1155/2021/6670709
48. Sharifi-Rad J, Dey A, Koirala N, et al. *Cinnamomum* species: bridging phytochemistry knowledge, pharmacological properties and toxicological safety for health benefits. Review. *Front Pharmacol.* **2021**;12(882). doi:10.3389/fphar.2021.600139
49. Rhayour K, Bouchikhi T, Tantaoui-Elaraki A, Sendide K, Remmal A. The mechanism of bactericidal action of oregano and clove essential oils and of their phenolic major components on *Escherichia coli* and *Bacillus subtilis*. *J Essent Oil Res.* **2003**;15(4):286–292. doi:10.1080/10412905.2003.9712144
50. Helander IM, Alakomi H-L, Latva-Kala K, et al. Characterization of the action of selected essential oil components on gram-negative bacteria. *J Agri Food Chem.* **1998**;46(9):3590–3595. doi:10.1021/jf980154m
51. Subash Babu P, Prabuseenivasan S, Ignacimuthu S. Cinnamaldehyde—a potential antidiabetic agent. *Phytomedicine.* **2007**;14(1):15–22. doi:10.1016/j.phymed.2006.11.005
52. Prasad KN, Yang B, Dong X, et al. Flavonoid contents and antioxidant activities from *Cinnamomum* species. *Innovative Food Sci Emerg Technol.* **2009**;10(4):627–632. doi:10.1016/j.ifset.2009.05.009
53. Kim DH, Kim CH, Kim MS, et al. Suppression of age-related inflammatory NF-kappaB activation by cinnamaldehyde. *Biogerontology.* **2007**;8(5):545–554. doi:10.1007/s10522-007-9098-2
54. Daker M, Lin VY, Akowuah GA, Yam MF, Ahmad M. Inhibitory effects of *Cinnamomum burmannii* Blume stem bark extract and trans-cinnamaldehyde on nasopharyngeal carcinoma cells; synergism with cisplatin. *Exp Ther Med.* **2013**;5(6):1701–1709. doi:10.3892/etm.2013.1041



55. Koppikar SJ, Choudhari AS, Suryavanshi SA, Kumari S, Chattopadhyay S, Kaul-Ghanekar R. Aqueous cinnamon extract (ACE-c) from the bark of *Cinnamomum cassia* causes apoptosis in human cervical cancer cell line (SiHa) through loss of mitochondrial membrane potential. *BMC Cancer*. 2010;10:210. doi:10.1186/1471-2407-10-210
56. Yadav S, Khurana JM. *Cinnamomum tamala* leaf extract-mediated green synthesis of Ag nanoparticles and their use in pyranopyrazles synthesis. *Chin J Catal* 2015;36(7):1042–1046. doi:10.1016/s1872-2067(15)60853-1
57. Maddinedi S, Mandal BK, Maddili SK. Biofabrication of size controllable silver nanoparticles – a green approach. *J Photochem Photobiol B Biol*. 2017;167:236–241. doi:10.1016/j.jphotobiol.2017.01.003
58. Aref MS, Salem SS. Bio-callsus synthesis of silver nanoparticles, characterization, and antibacterial activities via *Cinnamomum camphora* callus culture. *Biocatal Agric Biotechnol*. 2020;27:101689. doi:10.1016/j.bcab.2020.101689
59. Fatima M, Zaidi NU, Amraiz D, Afzal F. In vitro antiviral activity of *Cinnamomum cassia* and its nanoparticles against H7N3 influenza A virus. *J Microbiol Biotechnol*. 2016;26(1):151–159. doi:10.4014/jmb.1508.08024
60. Alwan SH, Al-Saeed MH. Biosynthesized silver nanoparticles (using *Cinnamomum zeylanicum* bark extract) improve the fertility status of rats with polycystic ovarian syndrome. *Biocatal Agric Biotechnol*. 2021;38:102217. doi:10.1016/j.bcab.2021.102217
61. Smitha SL, Philip D, Gopchandran KG. Green synthesis of gold nanoparticles using *Cinnamomum zeylanicum* leaf broth. *Spectrochim, Acta A Mol, Biomol, Spectrosc*. 2009;74(3):735–739. doi:10.1016/j.saa.2009.08.007
62. Chanda N, Shukla R, Zambre A, et al. An effective strategy for the synthesis of biocompatible gold nanoparticles using cinnamon phytochemicals for phantom CT imaging and photoacoustic detection of cancerous cells. *Pharm Res*. 2011;28(2):279–291. doi:10.1007/s11095-010-0276-6
63. ElMitwalli OS, Barakat OA, Daoud RM, Akhtar S, Henari FZ. Green synthesis of gold nanoparticles using cinnamon bark extract, characterization, and fluorescence activity in Au/eosin Y assemblies. *J Nanopart Res*. 2020;22(10):309. doi:10.1007/s11051-020-04983-8
64. Goyal D, Saini A, Saini GSS, Kumar R. Green synthesis of anisotropic gold nanoparticles using cinnamon with superior antibacterial activity. *Mater Res Express*. 2019;6(7):075043. doi:10.1088/2053-1591/ab15a6
65. Ling L, Jiang Y, Liu Y, et al. Role of gold nanoparticle from *Cinnamomum verum* against 1-methyl-4-phenyl-1, 2, 3, 6-tetrahydropyridine (MPTP) induced mice model. *J Photochem Photobiol B*. 2019;201(201):111657. doi:10.1016/j.jphotobiol.2019.111657
66. Huang J, Li Q, Sun D, et al. Biosynthesis of silver and gold nanoparticles by novel sundried *Cinnamomum camphora* leaf. *Nanotechnology*. 2007;18(10):105104. doi:10.1088/0957-4484/18/10/105104
67. Suresh T, Sivarajasekar N, Balasubramani K. Enhanced ultrasonic assisted biodiesel production from meat industry waste (pig tallow) using green copper oxide nanocatalyst: comparison of response surface and neural network modelling. *Renew Energy*. 2021;164:897–907. doi:10.1016/j.renene.2020.09.112
68. Kamran U, Bhatti HN, Iqbal M, Jamil S, Zahid M. Biogenic synthesis, characterization and investigation of photocatalytic and antimicrobial activity of manganese nanoparticles synthesized from *Cinnamomum verum* bark extract. *J Mol Struct*. 2019;1179:532–539. doi:10.1016/j.molstruc.2018.11.006
69. Agarwal H, Nakara A, Menon S, Shanmugam V. Eco-friendly synthesis of zinc oxide nanoparticles using *Cinnamomum tamala* leaf extract and its promising effect towards the antibacterial activity. *J Drug Delivery Sci Technol*. 2019;53:101212. doi:10.1016/j.jddst.2019.101212
70. Pillai AM, Sivasankarapillai VS, Rahdar A, et al. Green synthesis and characterization of zinc oxide nanoparticles with antibacterial and antifungal activity. *J Mol Struct*. 2020;1211:128107. doi:10.1016/j.molstruc.2020.128107
71. Maheswari P, Ponnusamy S, Harish S, Muthamizhchelvan C, Hayakawa Y. Syntheses and characterization of *Syzygium aromaticum*, *Elettaria cardamomum* and *Cinnamomum verum* modified TiO<sub>2</sub> and their biological applications. *Mater Sci Semicond Process*. 2020;105:104724. doi:10.1016/j.mssp.2019.104724
72. Mamaghani M, Hossein Nia R. A review on the recent multicomponent synthesis of pyranopyrazoles. *Polycyclic Aromatic Compounds*. 2021;41(2):223–291. doi:10.1080/10406638.2019.1584576
73. Gao G, Ze Y, Li B, et al. Ovarian dysfunction and gene-expressed characteristics of female mice caused by long-term exposure to titanium dioxide nanoparticles. *J Hazard Mater*. 2012;243:19–27. doi:10.1016/j.jhazmat.2012.08.049
74. Hou -C-C, Zhu J-Q. Nanoparticles and female reproductive system: how do nanoparticles affect oogenesis and embryonic development. *Oncotarget*. 2017;8(65):109799–109817. doi:10.18632/oncotarget.19087
75. Teimuri-mofrad R, Hadi R, Tahmasebi B, Farhoudian S, Mehravar M, Nasiri R. Green synthesis of gold nanoparticles using plant extract: mini-review. *Nanochem Res*. 2017;2(1):8–19. doi:10.22036/ncr.2017.01.002
76. Dubey SP, Lahtinen M, Sillanpää M. Green synthesis and characterizations of silver and gold nanoparticles using leaf extract of *Rosa rugosa*. *Colloids Surf A*. 2010;364(1):34–41. doi:10.1016/j.colsurfa.2010.04.023
77. Beheshtkhoo N, Kouhbanani MAJ, Savardashtaki A, Amani AM, Taghizadeh S. Green synthesis of iron oxide nanoparticles by aqueous leaf extract of *Daphne mezereum* as a novel dye removing material. *Appl Phys A*. 2018;124(5):363. doi:10.1007/s00339-018-1782-3
78. Geng R, Luong HM, Pham MT, et al. Magnetically tunable organic semiconductors with superparamagnetic nanoparticles. 10.1039/C9MH00265K. *Mater Horizons*. 2019;6(9):1913–1922. doi:10.1039/C9MH00265K
79. Yousefi M, Gholamian F, Ghanbari D, Salavati-Niasari M. Polymeric nanocomposite materials: preparation and characterization of star-shaped PbS nanocrystals and their influence on the thermal stability of acrylonitrile-butadiene-styrene (ABS) copolymer. *Polyhedron*. 2011;30(6):1055–1060. doi:10.1016/j.poly.2011.01.012
80. Masjedi-Arani M, Salavati-Niasari M. A simple sonochemical approach for synthesis and characterization of Zn<sub>2</sub>SiO<sub>4</sub> nanostructures. *Ultrason Sonochem*. 2016;29:226–235. doi:10.1016/j.ultsonch.2015.09.020
81. Duguet E, Vasseur S, Mornet S, Devoisselle JM. Magnetic nanoparticles and their applications in medicine. *Nanomedicine*. 2006;1(2):157–168. doi:10.2217/17435889.1.2.157
82. Nadi A, Jamoudi Sbai S, Bentiss A, Belaiche M, Briche S, Gmouh S. Application of Fe<sub>3</sub>O<sub>4</sub> nanoparticles on cotton fabrics by the Pad-Dry-Cure process for the elaboration of magnetic and conductive textiles. *IOP Conf Ser Mater Sci Eng*. 2020;827(1):012021. doi:10.1088/1757-899x/827/1/012021
83. Nanda T, Alobaid M, Rege K. Iron oxide nanoparticles for tissue repair and regeneration. *Nano LIFE*. 2021;11(01):2030001. doi:10.1142/s1793984420300010

84. Vangijzegem T, Stanicki D, Laurent S. Magnetic iron oxide nanoparticles for drug delivery: applications and characteristics. *Expert Opin Drug Deliv.* **2019**;16(1):69–78. doi:10.1080/17425247.2019.1554647
85. Guler E, Demir B, Guler B, Demirkol DO, Timur S. Chapter 3 - Biofunctionalized nanomaterials for targeting cancer cells. In: Fica A, Grumezescu AM, editors. *Nanostructures for Cancer Therapy*. Elsevier; **2017**:51–86.
86. Kaminski MD, Rosengart AJ. Detoxification of blood using injectable magnetic nanospheres: a conceptual technology description. *J Magn Magn Mater.* **2005**;293(1):398–403. doi:10.1016/j.jmmm.2005.02.055
87. Naseem T, Farrukh MA. Antibacterial activity of green synthesis of iron nanoparticles using *Lawsonia inermis* and *Gardenia jasminoides* leaves extract. *J Chem.* **2015**;912342. doi:10.1155/2015/912342
88. Mohan Kumar K, Mandal BK, Siva Kumar K, Sreedhara Reddy P, Sreedhar B. Biobased green method to synthesise palladium and iron nanoparticles using *Terminalia chebula* aqueous extract. *Spectrochim Acta A Mo Biomol Spectrosc.* **2013**;102:128–133. doi:10.1016/j.saa.2012.10.015
89. Rana A, Yadav K, Jagadevan S. A comprehensive review on green synthesis of nature-inspired metal nanoparticles: mechanism, application and toxicity. *J Cleaner Prod.* **2020**;272:122880. doi:10.1016/j.jclepro.2020.122880
90. Suman R, Javaid M, Haleem A, Vaishya R, Bahl S, Nandan D. Sustainability of coronavirus on different surfaces. *J Clin Exp Hepatol.* **2020**;10(4):386–390. doi:10.1016/j.jceh.2020.04.020
91. Ferro C, Florindo HF, Santos HA. Selenium nanoparticles for biomedical applications: from development and characterization to therapeutics. *Adv Healthc Mater.* **2021**;10(16):e2100598. doi:10.1002/adhm.202100598
92. Wadhvani SA, Shedbalkar UU, Singh R, Chopade BA. Biogenic selenium nanoparticles: current status and future prospects. *Appl Microbiol Biotechnol.* **2016**;100(6):2555–2566. doi:10.1007/s00253-016-7300-7
93. Hosnedlova B, Kepinska M, Skalickova S, et al. Nano-selenium and its nanomedicine applications: a critical review. *Int J Nanomed.* **2018**;13:2107–2128. doi:10.2147/ijn.S157541
94. Maiyo F, Singh M. Selenium nanoparticles: potential in cancer gene and drug delivery. *Nanomedicine.* **2017**;12(9):1075–1089. doi:10.2217/nnm-2017-0024
95. Gautam PK, Kumar S, Tomar MS, et al. Selenium nanoparticles induce suppressed function of tumor associated macrophages and inhibit Dalton's lymphoma proliferation. *Biochem Biophys Rep.* **2017**;12:172–184. doi:10.1016/j.bbrep.2017.09.005
96. Hu Y, Liu T, Li J, et al. Selenium nanoparticles as new strategy to potentiate  $\gamma\delta$  T cell anti-tumor cytotoxicity through upregulation of tubulin- $\alpha$  acetylation. *Biomaterials.* **2019**;222:119397. doi:10.1016/j.biomaterials.2019.119397
97. Khurana A, Tekula S, Saifi MA, Venkatesh P, Godugu C. Therapeutic applications of selenium nanoparticles. *Biomed Pharmacother.* **2019**;111:802–812. doi:10.1016/j.biopha.2018.12.146
98. Pi J, Shen L, Yang E, et al. Macrophage-targeted isoniazid-selenium nanoparticles promote antimicrobial immunity and synergize bactericidal destruction of *Tuberculosis* bacilli. *Angew Chem Int Ed Engl.* **2020**;59(8):3226–3234. doi:10.1002/anie.201912122
99. Al-Saggaf MS, Tayel AA, Ghobashy MOI, Alotaibi MA, Alghuthaymi MA, Moussa SH. Phytosynthesis of selenium nanoparticles using the *costus* extract for bactericidal application against foodborne pathogens. *Green Process Synthesis.* **2020**;9(1):477–487. doi:10.1515/gps-2020-0038
100. Zonaro E, Lampis S, Turner RJ, Qazi SJ, Vallini G. Biogenic selenium and tellurium nanoparticles synthesized by environmental microbial isolates efficaciously inhibit bacterial planktonic cultures and biofilms. *Front Microbiol.* **2015**;6:584. doi:10.3389/fmicb.2015.00584
101. Huang X, Chen X, Chen Q, Yu Q, Sun D, Liu J. Investigation of functional selenium nanoparticles as potent antimicrobial agents against superbugs. *Acta Biomater.* **2016**;30:397–407. doi:10.1016/j.actbio.2015.10.041
102. Iqbal H, Razzaq A, Uzair B, et al. Breast cancer inhibition by biosynthesized titanium dioxide nanoparticles is comparable to free doxorubicin but appeared safer in BALB/c mice. *Materials.* **2021**;14(12):3155. doi:10.3390/ma14123155
103. Ranjan S, Ramalingam C. Titanium dioxide nanoparticles induce bacterial membrane rupture by reactive oxygen species generation. *Environ Chem Lett* **2016**;14(4):487–494. doi:10.1007/s10311-016-0586-y
104. Nasikhudin DM, Kusumaatmaja A, Triyana K. Study on photocatalytic properties of TiO<sub>2</sub> nanoparticle in various pH condition. *J Physics.* **2018**;1011:012069. doi:10.1088/1742-6596/1011/1/012069
105. Alishah H, Pourseyedi S, Ebrahimipour SY, Mahani SE, Rafiei N. Green synthesis of starch-mediated CuO nanoparticles: preparation, characterization, antimicrobial activities and in vitro MTT assay against MCF-7 cell line. *Rendiconti Lincei.* **2017**;28(1):65–71. doi:10.1007/s12210-016-0574-y
106. Dutta A, Chakraborty A. Cinnamon in anticancer armamentarium: a molecular approach. *J Toxicol.* **2018**;2018:8978731. doi:10.1155/2018/8978731

## Nanotechnology, Science and Applications

### Publish your work in this journal

Nanotechnology, Science and Applications is an international, peer-reviewed, open access journal that focuses on the science of nanotechnology in a wide range of industrial and academic applications. It is characterized by the rapid reporting across all sectors, including engineering, optics, bio-medicine, cosmetics, textiles, resource sustainability and science. Applied research into nano-materials, particles, nano-structures and fabrication, diagnostics and analytics, drug delivery and toxicology constitute the primary direction of the journal. The manuscript management system is completely online and includes a very quick and fair peer-review system, which is all easy to use. Visit <http://www.dovepress.com/testimonials.php> to read real quotes from published authors.

Submit your manuscript here: <https://www.dovepress.com/nanotechnology-science-and-applications-journal>

**Dovepress**  
Taylor & Francis Group